ATLAS and CMS multiboson measurements

M. LIZZO

ON BEHALF OF THE ATLAS AND CMS COLLABORATIONS

Introduction

Multiboson measurements span several order of magnitudes in SM cross sections, from inclusive production ($\sim 10 - 100$ pb) to rare VBS processes (~ 1 fb), and both the ATLAS and CMS collaborations have covered a wide range of physics results in this sector

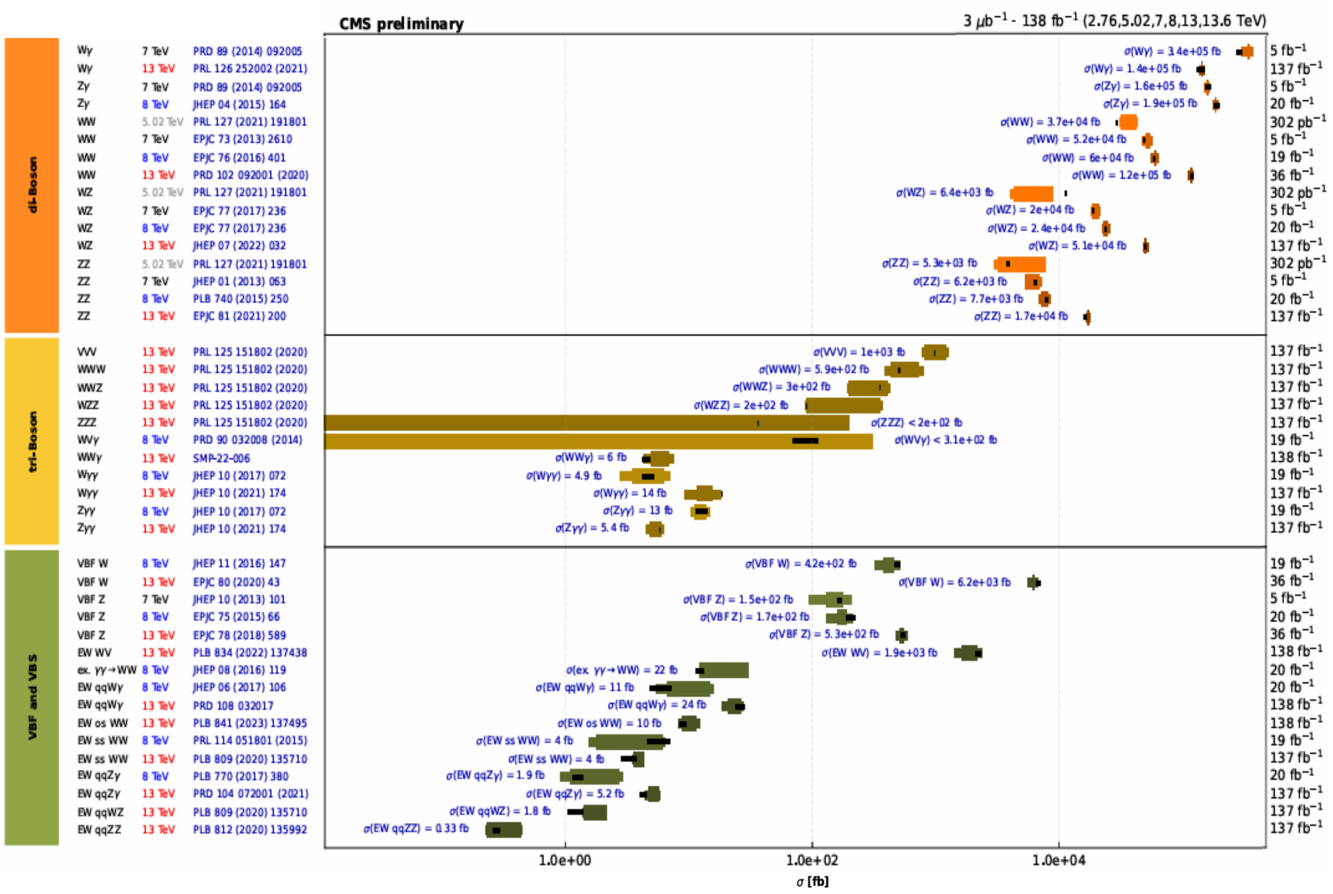

Standard Model Production Cross Section Measurements II

ATLAS Preliminary

$\sqrt{s}$ = 7, 8, 13, 13.6 TeV

Status: October 2023

Model	E_{CM} [TeV]	$\int\mathcal{L}\,dt$[fb^{-1}]	Measurement	Theory	Reference
WW	13	36.1	$\sigma = 130.04 \pm 1.7 \pm 10.6$ pb	$\sigma = 128.4 + 3.2 - 2.9$ pb (NNLO)	EPJC 79 (2019) 884
WW	8	20.3	$\sigma = 68.2 \pm 1.2 \pm 4.6$ pb	$\sigma = 65 + 1.2 - 1.1$ pb (NNLO)	PLB 763, 114 (2016)
WW	7	4.6	$\sigma = 51.9 \pm 2 \pm 4.4$ pb	$\sigma = 49.04 + 1.03 - 0.88$ pb (NNLO)	PRD 87 (2013) 112001, PRL 113 (2014) 212001
$\sigma^{fid}(WW\to e\mu)$ [$n_{jet}\geq 0$]	7	4.6	$\sigma = 563 \pm 28 + 79 - 85$ fb	$\sigma = 536 \pm 29$ fb (MCFM)	PRD 91 (2015) 052005
$\sigma^{fid}(WW\to e\mu)$ [$n_{jet}=1$]	8	20.3	$\sigma = 136 \pm 6 \pm 14.3$ fb	$\sigma = 141 \pm 30$ fb (NLO)	PLB 763 (2016) 114
$\sigma^{fid}(WW\to e\mu)$ [$n_{jet}\geq 1$]	13	139	$\sigma = 258 \pm 4 \pm 25$ fb	$\sigma = 279 \pm 2$ fb (NLO)	ATL-COM-PHYS-2020-574
$\sigma^{fid}(WW\to e\mu)$ [$n_{jet}=0$]	13	36.1	$\sigma = 379.1 \pm 5 \pm 27$ fb	$\sigma = 347 \pm 20$ fb (NNLO + NLO EW)	EPJC 79 (2019) 884
$\sigma^{fid}(WW\to e\mu)$ [$n_{jet}=0$]	8	20.3	$\sigma = 374 \pm 7 + 26 - 24$ fb	$\sigma = 346 \pm 19$ fb (approx. NNLO)	JHEP 09 (2016) 029
$\sigma^{fid}(WW\to e\mu)$ [$n_{jet}=0$]	7	4.6	$\sigma = 262.3 \pm 12.3 \pm 23.1$ fb	$\sigma = 231.4 \pm 15.7$ fb (MCFM)	PRD 87, 112001 (2013)
$\sigma^{fid}(WW\to \mu\mu)$ [$n_{jet}=0$]	8	20.3	$\sigma = 80.2 + 3.3 - 3.2 + 6.6 - 5.7$ fb	$\sigma = 71.2 \pm 4$ fb (NNLO)	JHEP 09 (2016) 029
$\sigma^{fid}(WW\to \mu\mu)$ [$n_{jet}=0$]	7	4.6	$\sigma = 73.9 \pm 5.9 \pm 7.5$ fb	$\sigma = 58.9 \pm 4$ fb (MCFM)	PRD 87, 112001 (2013)
$\sigma^{fid}(WW\to ee)$ [$n_{jet}=0$]	8	20.3	$\sigma = 73.4 + 4.2 - 4.1 + 6.7 - 5.8$ fb	$\sigma = 65.5 \pm 3.6$ fb (NNLO)	JHEP 09 (2016) 029
$\sigma^{fid}(WW\to ee)$ [$n_{jet}=0$]	7	4.6	$\sigma = 56.4 \pm 6.8 \pm 10$ fb	$\sigma = 54.6 \pm 3.7$ fb (MCFM)	PRD 87, 112001 (2013)
$\gamma\gamma\to WW\to e\mu X$	13	139	$\sigma = 3.13 \pm 0.31 \pm 0.28$ fb	$\sigma = 3.5 \pm 1$ fb (MG5_aMCNLO+Pythia8 × Surv. Fact (0.82))	PLB 816 (2021) 136190
$\gamma\gamma\to WW\to e\mu X$	8	20.2	$\sigma = 6.9 \pm 2.2 \pm 1.4$ fb	$\sigma = 4.4 \pm 0.3$ fb (HERWIG++)	PRD 94 (2016) 032011
$\sigma^{fid}(W^\pm W^\pm jj)$ EWK	13	139	$\sigma = 2.92 \pm 0.22 \pm 0.19$ fb	$\sigma = 2.53 + 0.22 - 0.19$ fb (Madgraph5 + aMCNLO)	Target journal JHEP
$\sigma^{fid}(W^\pm W^\pm jj)$ EWK	8	20.3	$\sigma = 1.5 \pm 0.5 \pm 0.2$ fb	$\sigma = 0.95 \pm 0.06$ fb (PowhegBox)	PRD 96, 012007 (2017)
WZ	13	36.1	$\sigma = 51 \pm 0.8 \pm 2.3$ pb	$\sigma = 49.1 + 1.1 - 1$ pb (MATRIX (NNLO))	EPJC 79 (2019) 535
WZ	8	20.3	$\sigma = 24.3 \pm 0.6 \pm 0.9$ pb	$\sigma = 23.92 \pm 0.4$ pb (MATRIX (NNLO))	PRD 93, 092004 (2016)
WZ	7	4.6	$\sigma = 19 + 1.4 - 1.3 \pm 1$ pb	$\sigma = 19.34 + 0.3 - 0.4$ pb (MATRIX (NNLO))	EPJC 72 (2012) 2173
$\sigma^{fid}(WZ \to \ell\nu\ell\ell)$	13	36.1	$\sigma = 255 \pm 1 \pm 11$ fb	$\sigma = 246 + 6 - 5$ fb (MATRIX (NNLO))	EPJC 79 (2019) 535
$\sigma^{fid}(WZ \to \ell\nu\ell\ell)$	8	20.3	$\sigma = 140.4 \pm 3.8 \pm 4.6$ fb	$\sigma = 142.4 + 2.6 - 2.7$ fb (MCFM NLO)	PRD 93 (2016) 092004
$\sigma^{fid}(WZjj)$ EWK	13	36.1	$\sigma = 0.57 + 0.14 - 0.13 + 0.07 - 0.05$ fb	$\sigma = 0.32 \pm 0.03$ fb (Sherpa 2.2.2)	PLB 793 (92019) 469
$\sigma^{fid}(WZjj)$ EWK	8	20.3	$\sigma = 0.29 + 0.14 - 0.12 + 0.09 - 0.1$ fb	$\sigma = 0.13 \pm 0.01$ fb (VBFNLO)	PRD 93 (2016) 092004
$WW+WZ\to \ell\nu J$	8	20.2	$\sigma = 30 \pm 11 \pm 22$ fb	$\sigma = 58 \pm 15$ fb (MC@NLO)	EPJC 77 (2017) 563
ZZ	13.6	29.0	$\sigma = 16.9 \pm 0.7 \pm 0.7$ pb	$\sigma = 16.7 \pm 0.4$ pb (Matrix (NNLO) & Sherpa (NLO))	ATLAS-CONF-2023-062
ZZ	13	36.1	$\sigma = 17.3 \pm 0.6 \pm 0.8$ pb	$\sigma = 16.9 + 0.6 - 0.5$ pb (Matrix (NNLO) & Sherpa (NLO))	PRD 97 (2018) 032005
ZZ	8	20.3	$\sigma = 7.3 \pm 0.4 + 0.4 - 0.3$ pb	$\sigma = 8.284 + 0.249 - 0.191$ pb (NNLO)	JHEP 01, 099 (2017)
ZZ	7	4.6	$\sigma = 6.7 \pm 0.7 + 0.5 - 0.4$ pb	$\sigma = 6.735 + 0.195 - 0.155$ pb (NNLO)	JHEP 03, 128 (2013), PLB 735 (2014) 311
$ZZ \to 4\ell$	8	20.3	$\sigma = 107 \pm 9 \pm 5$ fb	$\sigma = 104.9 \pm 1.7$ fb (Powheg)	PRL 112 (2014) 231806
$ZZ \to 4\ell$	7	4.5	$\sigma = 76 \pm 18 \pm 4$ fb	$\sigma = 90 \pm 1.6$ fb (Powheg)	PRL 112 (2014) 231806
$\sigma^{fid}(ZZ \to 4\ell)$	13	139	$\sigma = 49.3 \pm 0.8 \pm 1.1$ fb	$\sigma = 46 \pm 2.9$ fb (Sherpa (NLO))	JHEP 07 (2021) 005
$\sigma^{fid}(ZZ \to 4\ell)$	7	4.6	$\sigma = 25.4 + 3.3 - 3 + 1.6 - 1.4$ fb	$\sigma = 20.9 + 1.1 - 0.9$ fb (PowhegBox & gg2ZZ)	JHEP 03 (2013) 128
$\sigma^{fid}(ZZ^* \to 4\ell)$	13	139	$\sigma = 88.9 \pm 1.1 \pm 2.74$ fb	$\sigma = 86 \pm 5$ fb (Sherpa (NLO))	JHEP 07 (2021) 005
$\sigma^{fid}(ZZ^* \to 4\ell)$	8	20.3	$\sigma = 73 \pm 4 \pm 5$ fb	$\sigma = 65 \pm 4$ fb (PowhegBox norm. to NNLO & gg2ZZ)	PLB 753 (2016) 552-572
$\sigma^{fid}(ZZ^* \to 4\ell)$	7	4.6	$\sigma = 29.8 + 3.8 - 3.5 + 2.1 - 1.9$ fb	$\sigma = 25.6 + 1.3 - 1.1$ fb (PowhegBox & gg2ZZ)	JHEP 03 (2013) 128
$\sigma^{fid}(ZZjj)$ EWK	13	139	$\sigma = 0.82 \pm 0.18 \pm 0.11$ fb	$\sigma = 0.61 \pm 0.03$ fb (Sherpa 2.2.2)	Nature Phys. 19 (2023) 237
Wjj EWK (m_{jj} > 500 GeV)	8	20.2	$\sigma = 159 \pm 10 \pm 26$ fb	$\sigma = 198 \pm 12$ fb (Powheg+Pythia8 NLO)	EPJC 77 (2017) 474
Wjj EWK (m_{jj} > 500 GeV)	7	4.7	$\sigma = 144 \pm 23 \pm 26$ fb	$\sigma = 144 \pm 11$ fb (Powheg+Pythia8 NLO)	EPJC 77 (2017) 474
Zjj EWK	13	139	$\sigma = 37.4 \pm 3.5 \pm 5.5$ fb	$\sigma = 39.5 \pm 3.6$ fb (Herwig7+VBFNLO)	EPJC 81 (2021) 163
Zjj EWK	8	20.3	$\sigma = 10.7 \pm 0.9 \pm 1.9$ fb	$\sigma = 9.38 + 0.3 - 0.4$ fb (PowhegBox (NLO))	JHEP 04, 031 (2014)

$W^+W^- \rightarrow e^{\pm}\nu\mu^{\mp}\nu$ @13.6 TeV

(CMS)

Submitted to Phys. Lett. B

Physics motivation

- **W^+W^- production is sensitive to EW boson self-interaction terms, provides a powerful test of perturbative corrections in QCD and is one of the main background in Higgs boson searches and $t\bar{t}$ analyses**, therefore it is extremely important to precisely measure this process at hadron colliders, which must be well modeled by event generators

- The CMS collaboration has recently published the first measurement at $\sqrt{s} = 13.6\,\mathrm{TeV}$ of the inclusive and differential $W^+W^- \to e^{\pm}\nu\mu^{\mp}\nu$ production cross section sections, adding another point to the center-of-mass energy spectrum

- Analyzed data are taken from pp collisions recorded by the CMS experiment in 2022, which corresponds to an integrated luminosity of $\mathcal{L} = 34.8\ \mathrm{fb}^{-1}$

- The result is compared to the most-precise available theory predictions, including NNLO QCD and NLO EW corrections

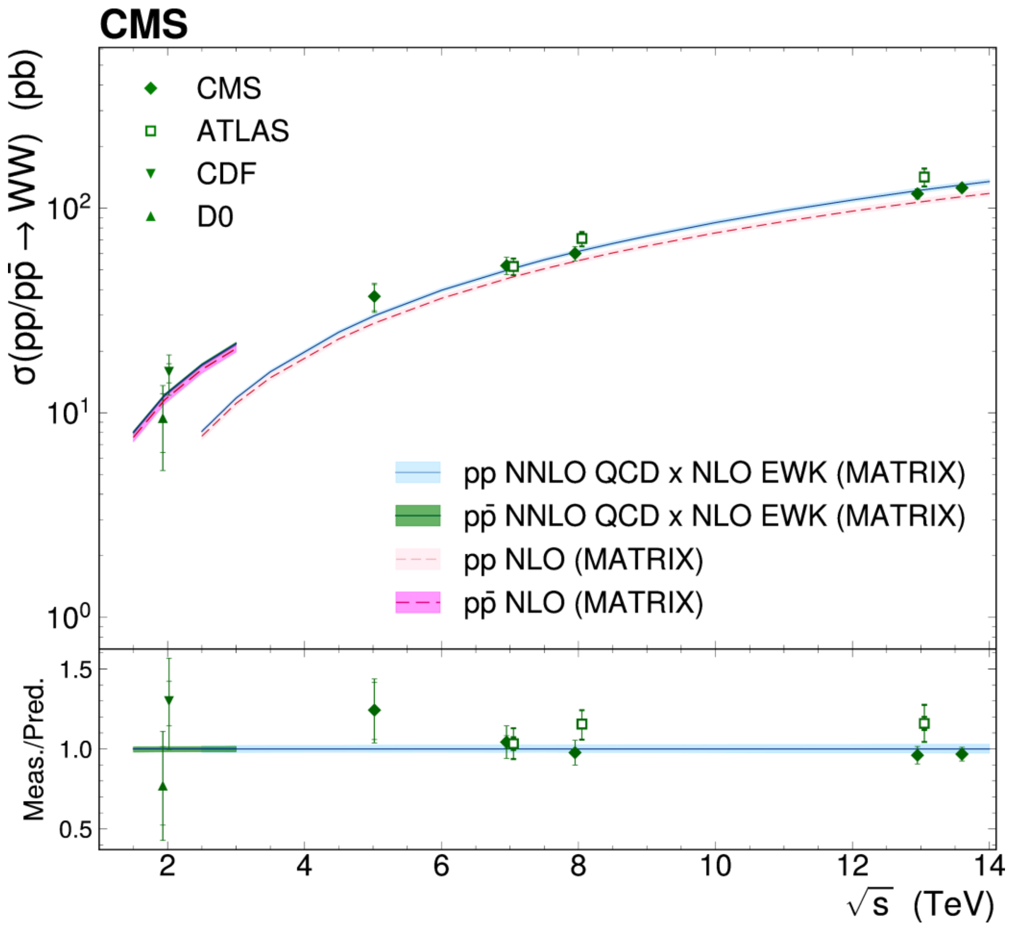

Analysis strategy

- Events are categorized as a function of the number of reconstructed jets, and the dominant background process is $t\bar{t}$, followed by non-prompt leptons and $Z \rightarrow \tau\tau$ productions

  → **dedicated control regions (CRs) are included in the fit procedure to constrain their normalizations**

Quantity	WW	One/two b tags	$Z \rightarrow \tau\tau$	Same-sign
Number of tight leptons		Strictly 2		
Additional loose leptons		0		
Lepton charges		Opposite		Same
$p_T^{\ell\,\max}$		>25 GeV		
$p_T^{\ell\,\min}$		>20 GeV		
$m_{\ell\ell}$	>85 GeV	>85 GeV	<85 GeV	>85 GeV
$p_T^{\ell\ell}$	—	—	<30 GeV	—
Number of b-tagged jets	0	1/2	0	0
N_j		$0/1/2/\geq 3$		

- Additional CRs with 3 and 4 leptons are added to estimate minor background contributions such as WZ and ZZ productions

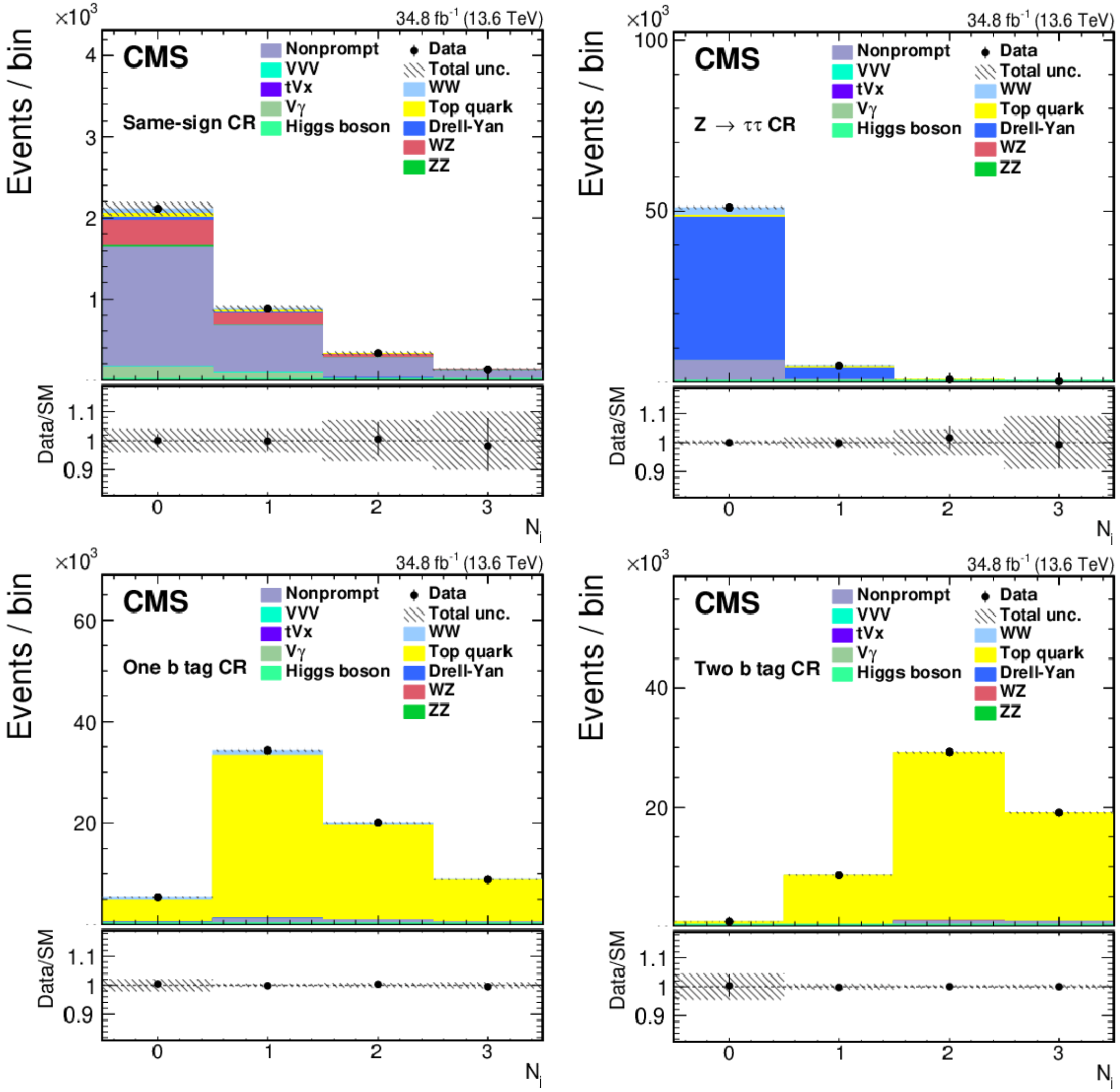

Fit strategy

- **Inclusive and *normalized* differential cross sections are simultaneously extracted from the fit**, where contributions from different generator-level bins (N_{jets}) are predicted by individual signal templates (signal extraction and unfolding embedded in the maximum likelihood fit)

$$s_i^{RECO} = \frac{\mu_{n_j=0}}{\mu_{fid}} S_{i,n_j=0}^{GEN} + \frac{\mu_{n_j=1}}{\mu_{fid}} S_{i,n_j=1}^{GEN} + \frac{1-\mu_{n_j=0}-\mu_{n_j=1}}{\mu_{fid}} S_{i,n_j\geq 2}^{GEN}$$

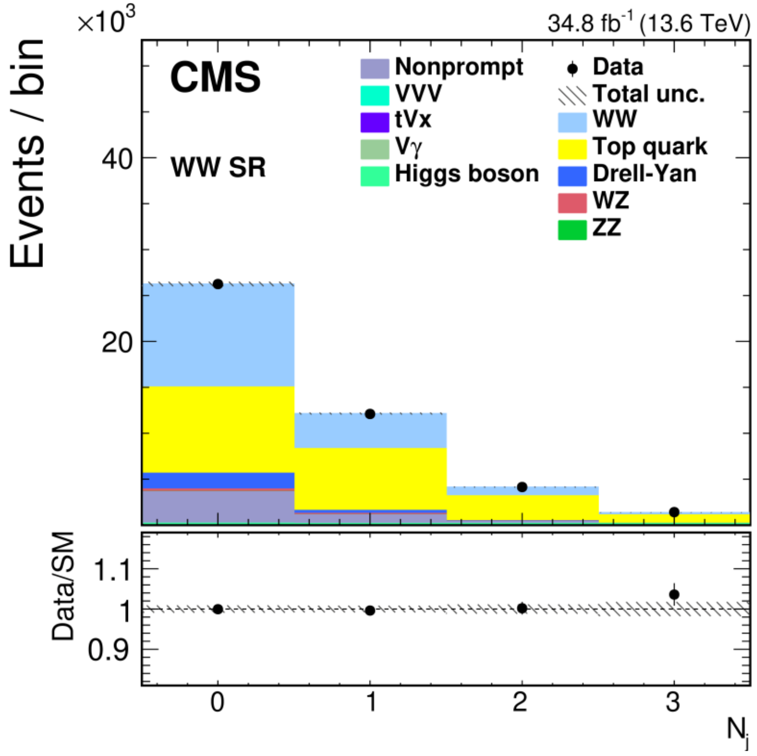

- **Improved fit strategy and techniques to reduce systematic uncertainties lead to a 25% increase in sensitivity** to W^+W^- production with respect to the CMS Run 2 measurement

Uncertainty source	(%)
Statistical	1.2
$t\bar{t}$ normalization	2.0
Drell–Yan normalization	1.4
$W\gamma^*$ normalization	0.4
Nonprompt leptons normalization	1.9
Lepton efficiencies	2.1
b tagging (b/c)	0.4
Mistag rate (q/g)	1.0
Jet energy scale and resolution	2.3
Pileup	0.4
Simulation and data control regions sample size	1.0
Total experimental systematic	4.6
QCD factorization and renormalization scales	0.4
Higher-order QCD corrections and p_T^{WW} distribution	1.4
PDF and α_S	0.4
Underlying event modeling	0.5
Total theoretical systematic	1.6
Integrated luminosity	2.7
Total	5.7

Run 2 to Run 3 →

Uncertainty source	$\Delta\mu$
Integrated luminosity	0.014
Lepton experimental	0.019
Jet experimental	0.008
b tagging	0.012
Nonprompt background	0.010
Limited sample size	0.017
Background normalization	0.018
Theory	0.011
Statistical	0.018
Total	0.044

Inclusive and differential results

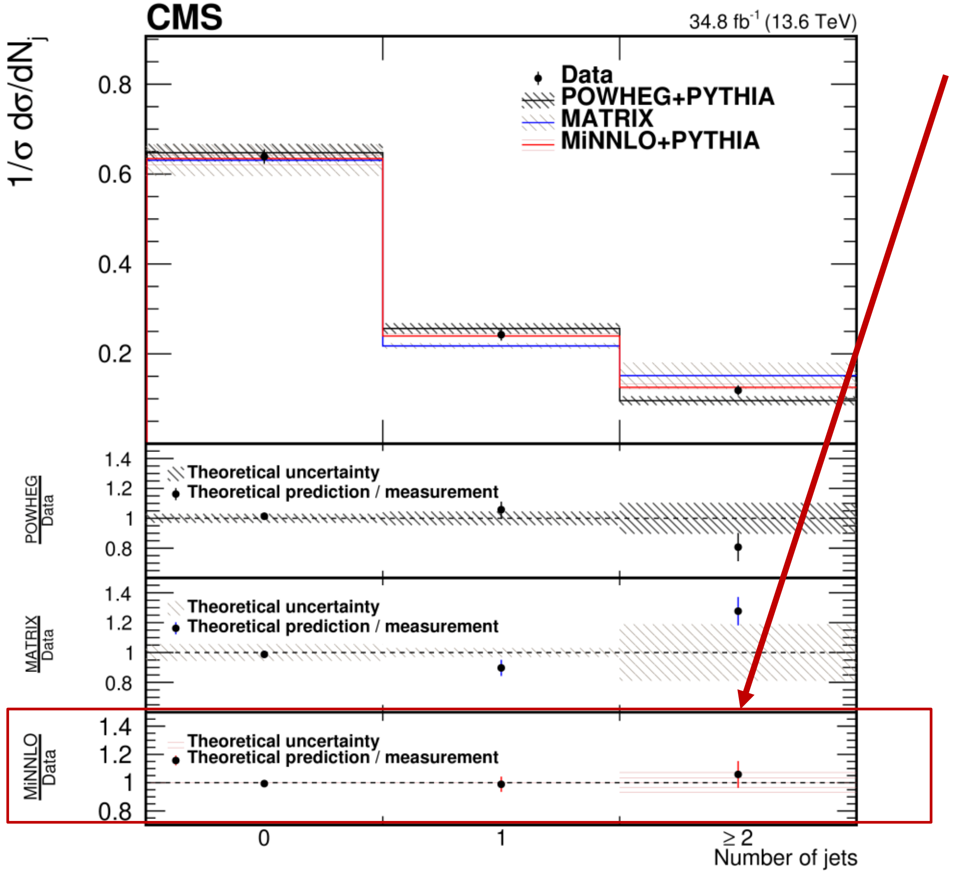

- **The Powheg MiNNLO prediction gives the best agreement with data**, showing a sizeable improvement with respect to other event generators

Fiducial volume definition

Variable	Requirement
Lepton origin	Direct decay of a prompt W boson
Lepton definition	Dressed leptons ($e^{\pm}\mu^{\mp}$)
Leading lepton p_T	$p_T^{\ell\,max} > 25\,GeV$
Trailing lepton p_T	$p_T^{\ell\,min} > 20\,GeV$
Additional leptons	0
$\lvert\eta\rvert$ of leptons	$\lvert\eta\rvert < 2.5$
Dilepton mass	$m_{\ell\ell} > 85\,GeV$
Jet p_T	$p_T^{j} > 30\,GeV$
$\lvert\eta\rvert$ of jets	$\lvert\eta^{j}\rvert < 2.5$
Jet-lepton removal	$\Delta R(j,\ell) > 0.4$

Inclusive cross section

$$\sigma_{inc} = 125.7 \pm 2.3(\text{stat}) \pm 4.8(\text{syst}) \pm 1.8(\text{lumi})\ \text{pb}$$
$$= 125.7 \pm 5.6\ \text{pb}$$

Observable	Expected	Observed
Cross section (fb)	$812 \pm 34\ (31, 15)$	$813 \pm 35\ (32, 15)$
0-jet fraction	$0.648 \pm 0.015\ (0.012, 0.009)$	$0.640 \pm 0.016\ (0.013, 0.009)$
1-jet fraction	$0.256 \pm 0.013\ (0.008, 0.010)$	$0.243 \pm 0.013\ (0.009, 0.010)$
$\geq$2-jet fraction	$0.096 \pm 0.011\ (0.008, 0.008)$	$0.119 \pm 0.011\ (0.008, 0.008)$

$ZZ \rightarrow 4\ell$ @13.6 TeV (ATLAS)

Phys. Lett. B 855 (2024) 138764

Physics motivation

- Despite being the rarest diboson process, **the production of two on-shell Z bosons is interesting to study because of its high signal-to-background ratio and sensitivity to anomalous neutral TGCs**

- The ATLAS collaboration reports the first measurement of ZZ production at $\sqrt{s} = 13.6\,\mathrm{TeV}$, providing inclusive and differential cross section sections as a function of two key variables $(m_{4\ell},\ p_T^{4\ell})$

- Analyzed data are taken from pp collisions recorded by the ATLAS experiment in 2022, which corresponds to an integrated luminosity of $\mathcal{L} = 29\ \mathrm{fb}^{-1}$

- Events are selected from the $ZZ \to 4\ell$ channel by considering all possible production modes:
    - $q\bar{q} \to ZZ$
    - $gg \to ZZ$
    - $gg \to (H^* \to)ZZ$
    - EW $qq \to ZZ + 2j$

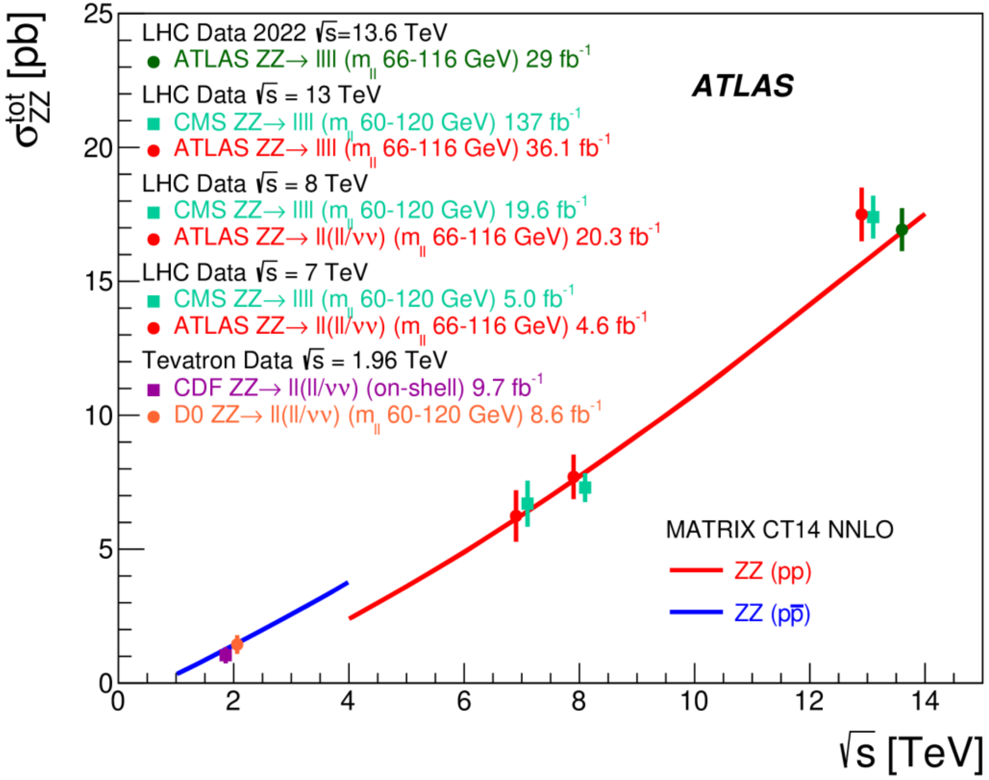

Analysis strategy

- Inclusive and differential cross sections are extracted from a pure signal region, where backgrounds give less than 5% of the total yield

- Irreducible contributions, namely $t\bar{t}Z$ and triboson production, are evaluated from MC simulation, whereas **non-prompt leptons are estimated with a data driven technique** ("fakeable-object method") and they are assigned a 30% conservative uncertainty

	Fiducial phase space	Total lepton phase space
Muon selection	Bare, $p_T > 5$ GeV, $\|\eta\| < 2.5$	Born
Electron selection	Dressed, $p_T > 7$ GeV, $\|\eta\| < 2.47$	Born
Four-lepton signature	≥ 2 SFOC pairs	≥ 2 SFOC pairs
Lepton kinematics	$p_T > 27/10$ GeV	
Lepton separation	$\Delta R(\ell_i, \ell_j) > 0.05$	
Low-mass $\ell^+\ell^-$ veto	$m_{ij} > 5$ GeV	$m_{ij} > 5$ GeV
Z mass window	$66 < m_{\ell\ell,1}, m_{\ell\ell,2} < 116$ GeV	$66 < m_{\ell\ell,1}, m_{\ell\ell,2} < 116$ GeV
ZZ on-shell	$m_{4l} > 180$ GeV	

$$\sigma_{fid} = \frac{N_{obs} - N_{bkg}}{\mathcal{L} \times C_{ZZ}} \qquad C_{ZZ} = \frac{N_{fid\,\&\,reco}}{N_{fid}} = 0.555 \pm 0.022$$

$$\sigma_{tot} = \frac{\sigma_{fid}}{\mathcal{BR}(ZZ \to 4\ell) A_{ZZ}} \qquad A_{ZZ} = \frac{N_{fid}}{N_{tot}} = 0.482 \pm 0.003$$

- The non-prompt leptons contribution in bins of the reco-level observable suffer from large statistical uncertainties

  → Smoothing procedure **is employed to reduce their impact in the result and get a more robust estimation**

	Measurement	MC prediction	MATRIX prediction
Fiducial	$36.7 \pm 1.6(\text{stat}) \pm 1.5(\text{syst}) \pm 0.8(\text{lumi})$ fb	$36.8\ ^{+4.3}_{-3.5}$ fb	36.5 ± 0.7 fb
Total	$16.8 \pm 0.7(\text{stat}) \pm 0.7(\text{syst}) \pm 0.4(\text{lumi})$ pb	$17.0\ ^{+1.9}_{-1.4}$ pb	16.7 ± 0.5 pb

Differential results

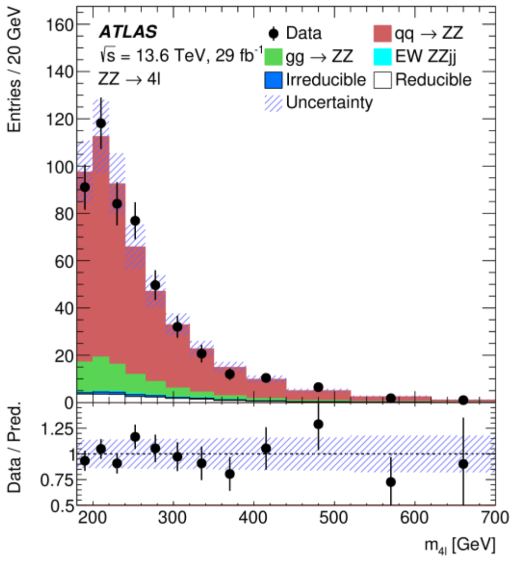

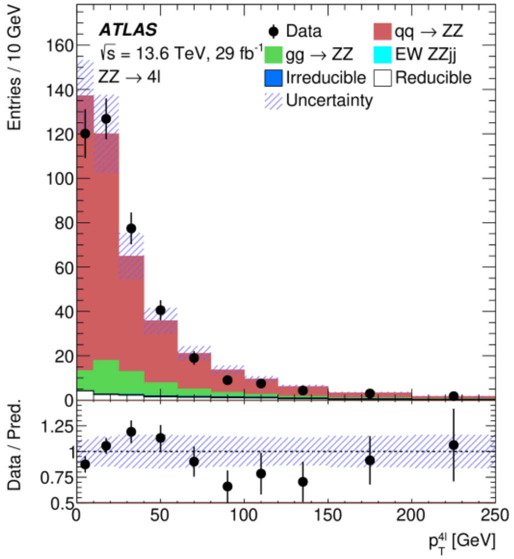

BAYESIAN UNFOLDING

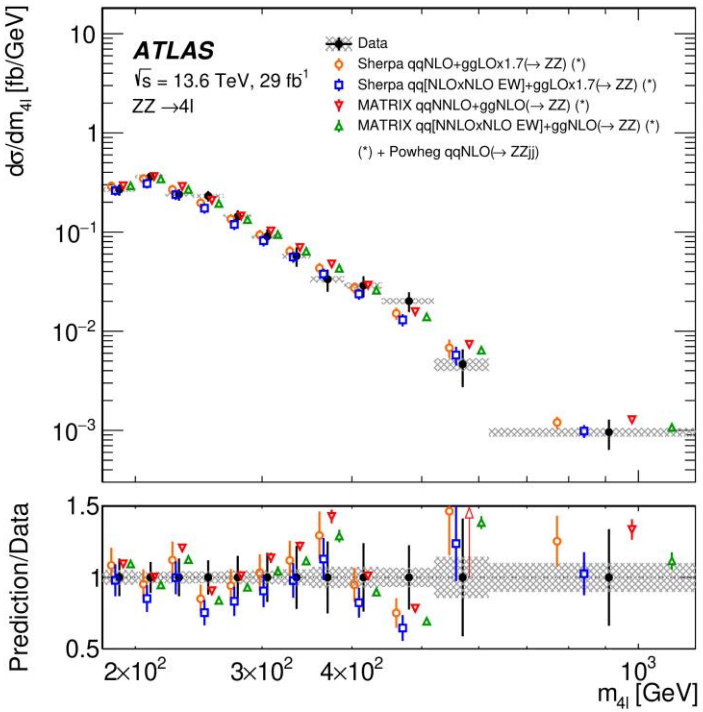

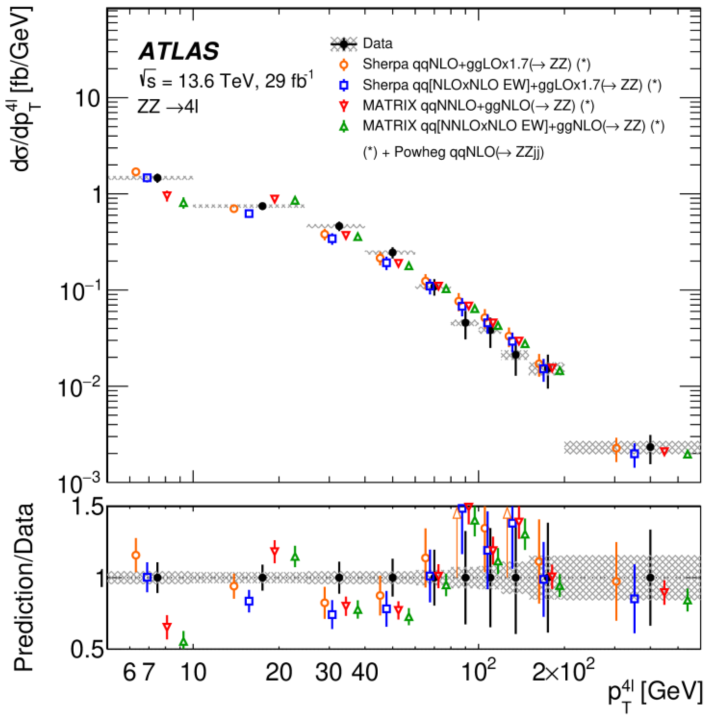

- **Bayesian unfolding** (two iterations) is performed to evaluate the response matrix, and the total bias is found to be below 1%
- **Each uncertainty in the signal process leads to a modification of the response matrix**, the largest contribution being the lepton efficiency

Source	Relative uncertainty(%)
Data statistical uncertainty	4.2
MC statistical uncertainty	0.3
Luminosity	2.2
Lepton momentum	0.2
Lepton efficiency	3.7
Background	1.6
Theoretical uncertainty	1.0
Total	6.3

VBS measurements @13 TeV

VBS analyses – where do we stand

VBS PROCESS	ATLAS	CMS
$WZjj \rightarrow 3\ell\nu jj$	JHEP 06 (2024) 192	PLB 809 (2020) 135710
$W^+W^-jj \rightarrow 2\ell2\nu jj$	ArXiv:2403.04869	PLB 841 (2023) 137495
$W(\rightarrow \ell\nu)\gamma jj$	ArXiv:2403.02809	PRD 108 (2023) 032017
$W^\pm W^\pm jj \rightarrow 2\ell2\nu jj$	JHEP 04 (2024) 026	PLB 812 (2020) 136018 PLB 809 (2020) 135710 Eur Phys J C 81 (2021) 723
$WVjj \rightarrow \ell\nu qqjj$	–	PLB 834 (2022) 137438
$W^\pm W^\pm jj \rightarrow \tau_h\ell\nu jj$	–	CDS:2867989
$Z(\rightarrow 2\ell)\gamma jj$	Phys. Lett. B 846 (2023) 138222	PRD 104 (2021) 072001
$Z(\rightarrow 2\nu)\gamma jj$	JHEP 06 (2023) 082	–
$ZZjj \rightarrow 4\ell jj$	Nature Phys. 19 (2023) 237	PLB 812 (2020) 135992

Both the ATLAS and CMS collaborations have published a **wide array of VBS results with full Run2 data , covering a lot of different final states and production modes**

I will be presenting the **latest VBS measurements**, trying to highlight common choices or differences whenever possible

Non-exhaustive talk, don't have time to go into the detail of every result

VBS topology

- **VBS processes share a similar kinematic topology**, regardless of what is the considered final state, which mainly affects the background contamination and trigger requirement
- The typical VBS configuration is often enough to suppress most of background processes, although sometimes machine learning techniques help in achieving a better sensitivty

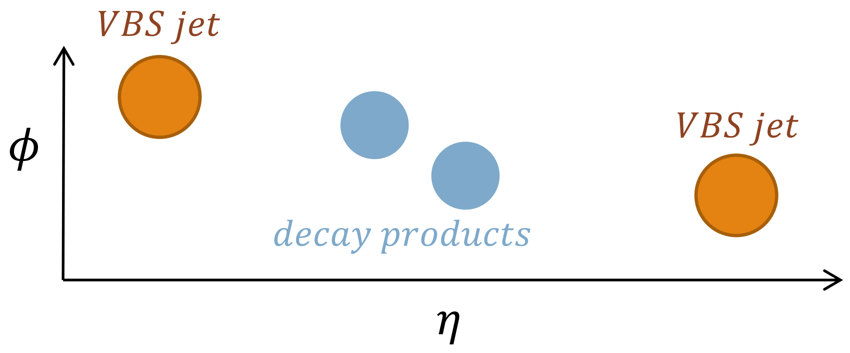

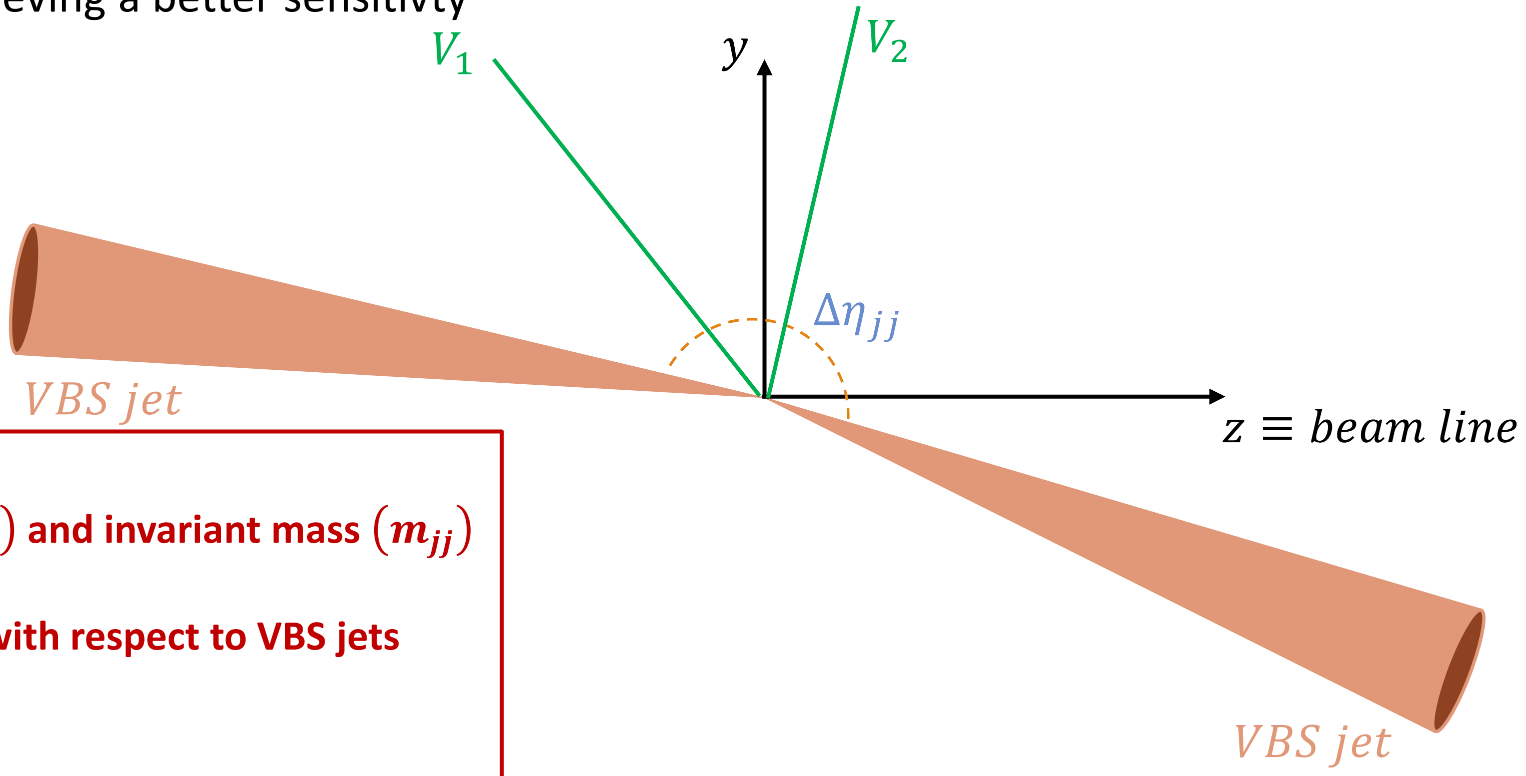

SIGNAL TOPOLOGY:

- **2 VBS jets with large pseudorapidity gap $(\Delta\eta_{jj})$ and invariant mass (m_{jj})**
- **$V = \{W, Z\}$ decay products emitted centrally with respect to VBS jets**
- **Little QCD activity between VBS jets**
- **Missing transverse energy due to the escaping neutrinos (if any)**

$W(\to \ell\nu)\gamma jj$

ATLAS: Submitted to EPJC

CMS: Phys. Rev. D 108 (2023) 032017

$W(\rightarrow \ell\nu)\gamma jj$

EW $W\gamma$

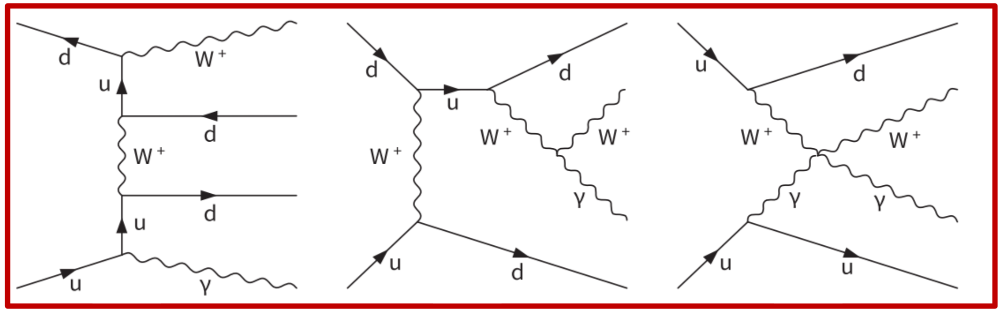

QCD $W\gamma$

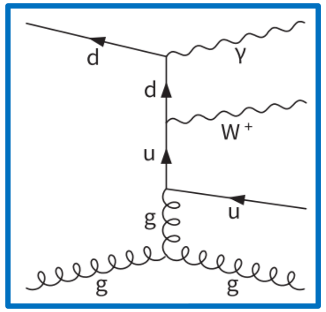

- VBS $W\gamma jj$ **fiducial + differential cross section** measurements and **aQGCs interpetretation** using Run 2 data

- **QCD $W\gamma jj$ production is the dominant background** of the analysis (interference with EWK $W\gamma jj$ taken into account)

- The signal reconstruction is based on:

  - **2 VBS jets**
  - **1 high-p_T and well-isolated lepton (either e or μ) + 1 high-p_T and well-isolated photon (γ)**
  - **Imbalance on the total transverse momentum (p_T^{miss})**

Jets mis-identified as either photons or leptons constitute another source of background **($W +$ jets and top quark processes)**

↓

The fraction of fake objects entering the signal region is estimated with a data-driven technique

Fiducial volume

CMS

- $p_T^\ell > 35$ GeV, $p_T^\gamma > 25$ GeV,
  $p_T^j > 50$ GeV, $E_T^{miss} > 30$ GeV
- $\Delta R(j,\ell) > 0.5, \Delta R(\gamma, j) > 0.5, \Delta R(j,j) > 0.5$
- $m_T^W \equiv \sqrt{2p_T^\ell E_T^{miss}(1-\cos\Delta\phi)} > 30$ GeV
- $|\Delta\eta_{jj}| > 2.5,\ m_{jj} > 500$ GeV

EVENT SELECTION

- $m_{W\gamma} > 100$ GeV, $\left|y_{l\gamma} - \frac{(y_{j_1}+y_{j_2})}{2}\right| < 1.2$
- $|\phi_{W\gamma} - \phi_{jj}| > 2, |m_{e\gamma} - m_Z| > 10$ GeV

aQGC LIMITS

- $m_{jj} > 800$ GeV
- $m_{W\gamma} > 150$ GeV, $p_T^\gamma > 100$ GeV

ATLAS

- $p_T^\ell > 30$ GeV, $p_T^\gamma > 22$ GeV,
  $p_T^j > 50$ GeV, $E_T^{miss} > 30$ GeV
- $\Delta R(j,\ell) > 0.2,\ \Delta R(\ell, j) > 0.4, \Delta R(\gamma, \ell/j) > 0.4$
- $m_T^W \equiv \sqrt{2p_T^\ell E_T^{miss}(1-\cos\Delta\phi)} > 30$ GeV
  $|m_{\ell\gamma} - m_Z| > 10$ GeV
- $|\Delta y_{jj}| > 2,\ m_{jj} > 500$ GeV

DIFFERENTIAL CROSS SECTION

- $\xi_{\ell\gamma} \equiv \left|\frac{\left(y_{l\gamma} - \frac{(y_{j_1}+y_{j_2})}{2}\right)}{y_{j_1}-y_{j_2}}\right| < 0.35$
- $m_{jj} > 1$ TeV, $N_{jets}^{gap} = 0$

Inclusive fiducial cross section

CMS

- m_{jj} vs $m_{\ell\gamma}$ distribution is fit to data in both the SR and CR
  → 6.0 σ observed (6.8 σ expected)

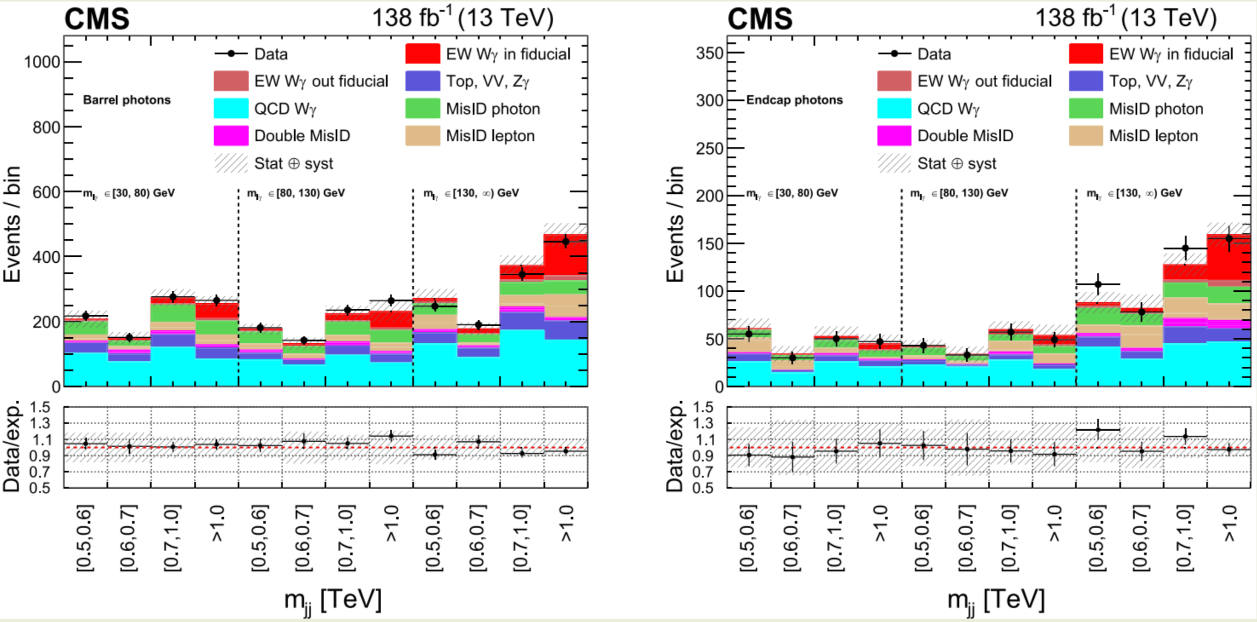

$$\sigma^{\text{fid}}_{\text{EW}} = 23.5 \pm 2.8\,(\text{stat})^{+1.9}_{-1.7}\,(\text{theo})^{+3.5}_{-3.4}\,(\text{syst})\ \text{fb}$$

$$\sigma^{\text{fid}}_{\text{EW+QCD}} = 113 \pm 2.0\,(\text{stat})^{+2.5}_{-2.3}\,(\text{theo})^{+13}_{-13}\,(\text{syst})\ \text{fb}$$

ATLAS

- NN output to extract the signal for the observation
  → ≫ 6 σ observed (6.3 σ expected)

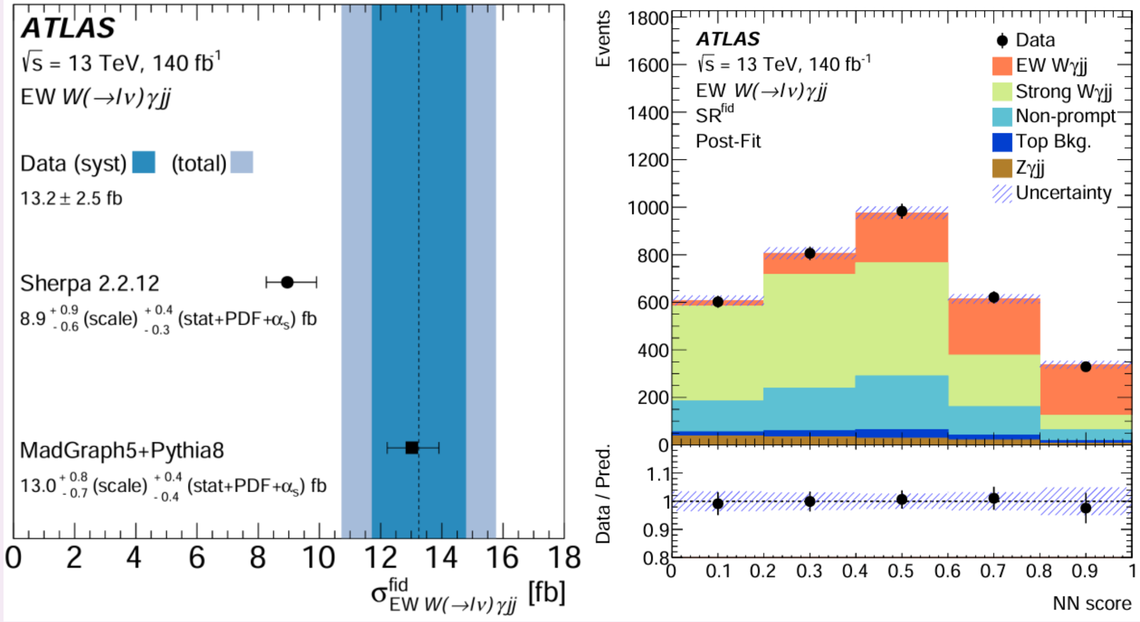

$$\boldsymbol{\sigma^{fid}_{EW} = 13.2 \pm 2.5\ \text{fb}}$$

Fiducial differential cross sections

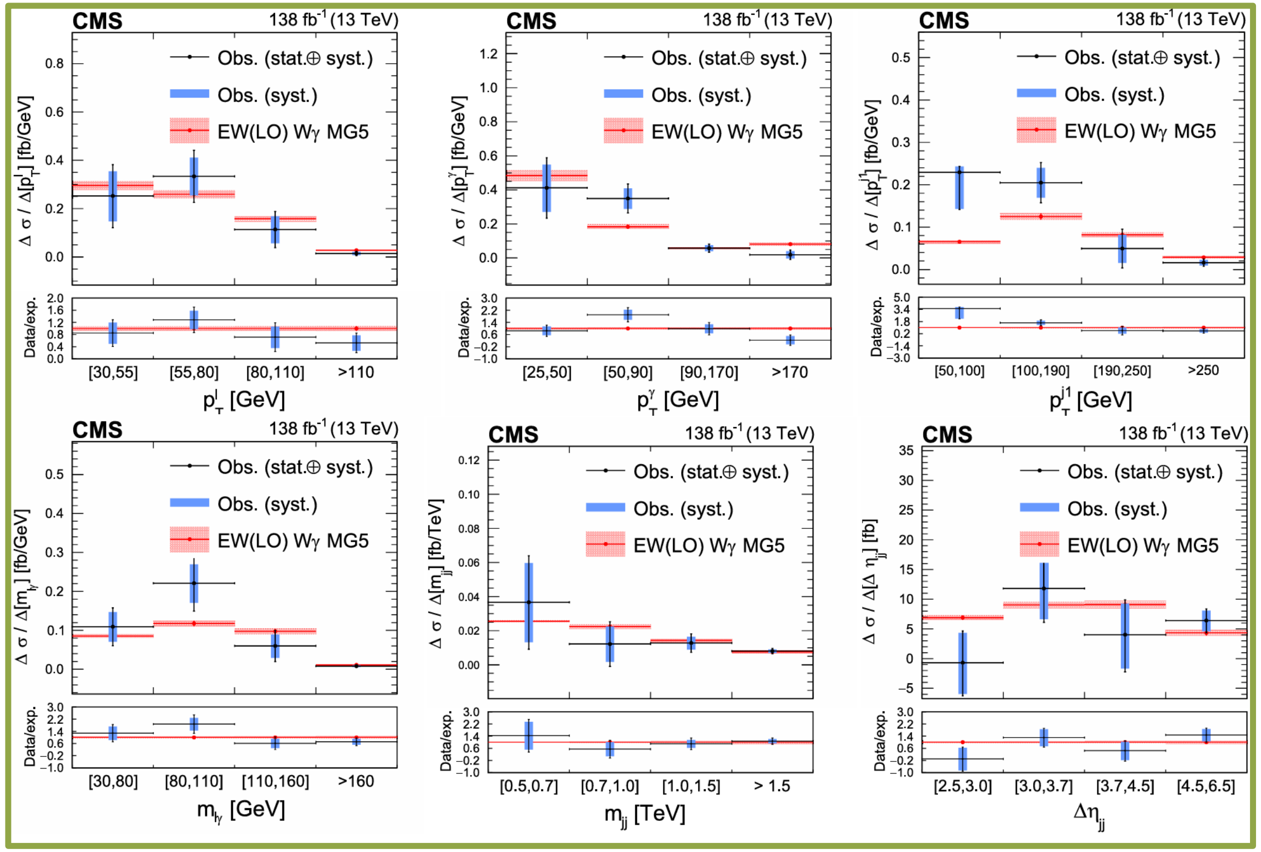

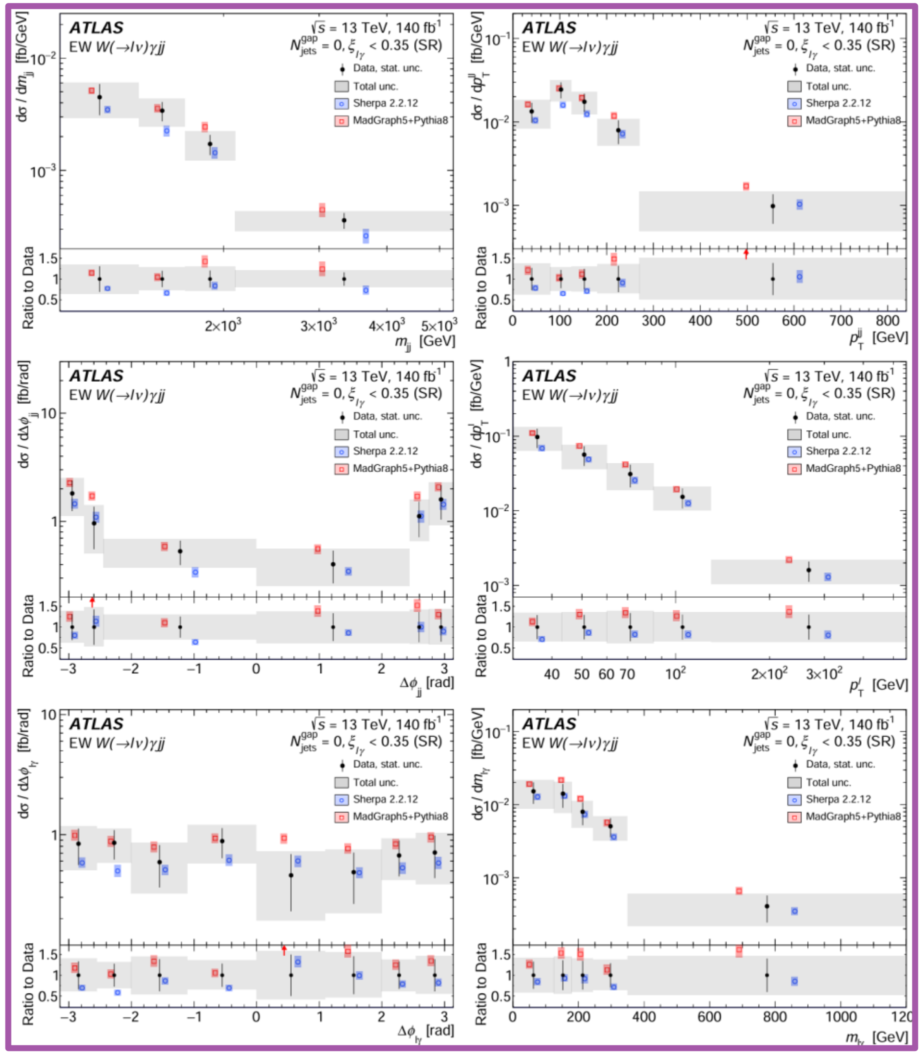

- **ATLAS extracts differential cross sections as a function of $\Delta\phi_{\ell\gamma}$ and $\Delta\phi_{jj}$ observables**, which are sensitive to CP-odd couplings
- **CMS measures both the EW and EW+QCD $W\gamma jj$ productions**

EFT interpretation (CMS)

- VBS processes are particularly sensitive to aQCGs, therefore the EW $W\gamma jj$ signal is suitable to constrain EFT dimension-8 operators (SM-BSM interference term included in the signal definition)
- Because BSM physics is expected to enhance the VBS production in the high-energy regime, **the invariant mass of the $W\gamma$ system $(m_{W\gamma})$ is used to extract limits on EFT operators**

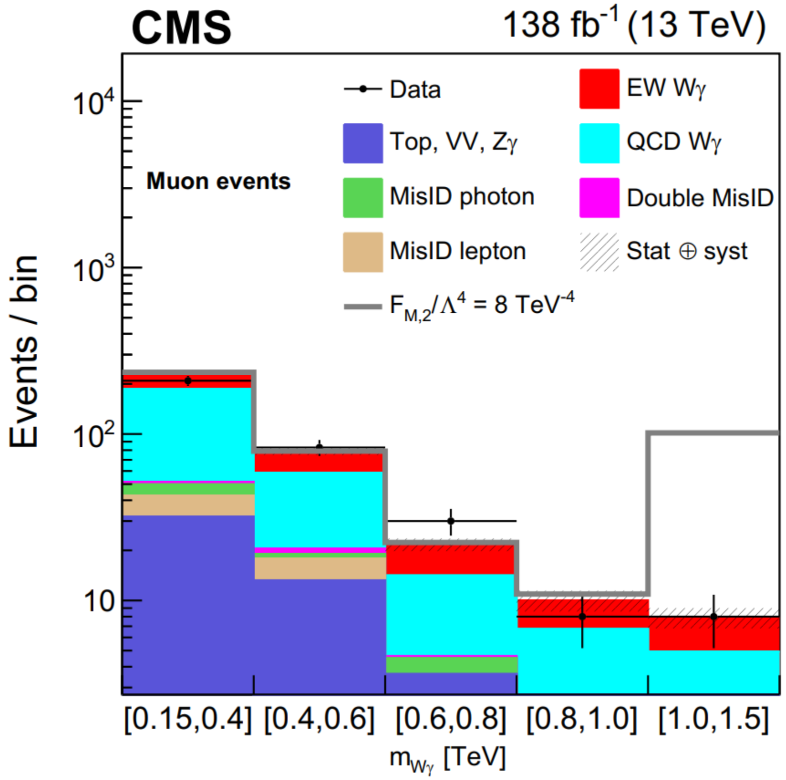

Expected limit	Observed limit	U_{bound}
$-5.1 < f_{M,0}/\Lambda^4 < 5.1$	$-5.6 < f_{M,0}/\Lambda^4 < 5.5$	1.7
$-7.1 < f_{M,1}/\Lambda^4 < 7.4$	$-7.8 < f_{M,1}/\Lambda^4 < 8.1$	2.1
$-1.8 < f_{M,2}/\Lambda^4 < 1.8$	$-1.9 < f_{M,2}/\Lambda^4 < 1.9$	2.0
$-2.5 < f_{M,3}/\Lambda^4 < 2.5$	$-2.7 < f_{M,3}/\Lambda^4 < 2.7$	2.7
$-3.3 < f_{M,4}/\Lambda^4 < 3.3$	$-3.7 < f_{M,4}/\Lambda^4 < 3.6$	2.3
$-3.4 < f_{M,5}/\Lambda^4 < 3.6$	$-3.9 < f_{M,5}/\Lambda^4 < 3.9$	2.7
$-13 < f_{M,7}/\Lambda^4 < 13$	$-14 < f_{M7}/\Lambda^4 < 14$	2.2
$-0.43 < f_{T,0}/\Lambda^4 < 0.51$	$-0.47 < f_{T,0}/\Lambda^4 < 0.51$	1.9
$-0.27 < f_{T,1}/\Lambda^4 < 0.31$	$-0.31 < f_{T,1}/\Lambda^4 < 0.34$	2.5
$-0.72 < f_{T,2}/\Lambda^4 < 0.92$	$-0.85 < f_{T,2}/\Lambda^4 < 1.0$	2.3
$-0.29 < f_{T,5}/\Lambda^4 < 0.31$	$-0.31 < f_{T,5}/\Lambda^4 < 0.33$	2.6
$-0.23 < f_{T,6}/\Lambda^4 < 0.25$	$-0.25 < f_{T,6}/\Lambda^4 < 0.27$	2.9
$-0.60 < f_{T,7}/\Lambda^4 < 0.68$	$-0.67 < f_{T,7}/\Lambda^4 < 0.73$	3.1

Unitarity bound limit derived for each operator (following the formulation discussed here)

Most stringent limits to date on aQGCs parameters

EFT interpretation (ATLAS)

- Limits on aQGCs are extracted by fitting either the p_T^{jj} or p_T^{ℓ} distribution to data and with or without the clipping technique described here
- Although CMS reports more stringent limits on mixed scalar operators, **ATLAS measures the very first limits on tensor-type operators f_{T3} and f_{T4}**

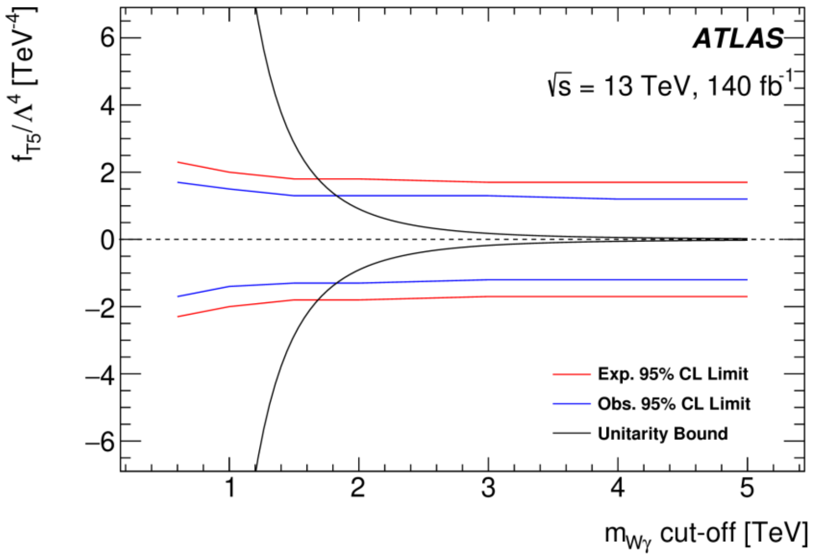

Cofficients [TeV^{-4}]	Observable	$M_{W\gamma}$ cut-off [TeV]	Expected [TeV^{-4}]	Observed [TeV^{-4}]
f_{T0}/Λ^4	p_T^{jj}	1.4	[-2.5, 2.6]	[-1.9, 1.9]
f_{T1}/Λ^4	p_T^{jj}	1.9	[-1.6, 1.6]	[-1.1, 1.2]
f_{T2}/Λ^4	p_T^{jj}	1.6	[-4.9, 5.3]	[-3.6, 4.0]
f_{T3}/Λ^4	p_T^{jj}	1.9	[-3.4, 3.6]	[-2.5, 2.7]
f_{T4}/Λ^4	p_T^{jj}	2.2	[-3.1, 3.1]	[-2.2, 2.3]
f_{T5}/Λ^4	p_T^{jj}	1.8	[-1.8, 1.8]	[-1.3, 1.3]
f_{T6}/Λ^4	p_T^{jj}	2.1	[-1.5, 1.5]	[-1.1, 1.1]
f_{T7}/Λ^4	p_T^{jj}	2.1	[-4.0, 4.1]	[-2.9, 3.0]
f_{M0}/Λ^4	p_T^{l}	1.1	[-45, 44]	[-32, 31]
f_{M1}/Λ^4	p_T^{l}	1.4	[-60, 62]	[-43, 44]
f_{M2}/Λ^4	p_T^{l}	1.4	[-15, 15]	[-11, 11]
f_{M3}/Λ^4	p_T^{l}	1.8	[-22, 22]	[-16, 16]
f_{M4}/Λ^4	p_T^{l}	1.5	[-28, 27]	[-20, 20]
f_{M5}/Λ^4	p_T^{l}	1.9	[-21, 23]	[-14, 17]
f_{M7}/Λ^4	p_T^{l}	1.5	[-100, 99]	[-73, 71]

Most stringent limits to date on aQGCs parameters

$$W^{\pm}W^{\pm}jj \rightarrow 2\ell 2\nu jj$$

ATLAS: JHEP 04 (2024) 026

CMS: PLB 809 (2020) 135710, Eur Phys J C 81 (2021) 723

$W^{\pm}W^{\pm}jj \rightarrow 2\ell 2\nu jj$

- **The EW $W^{\pm}W^{\pm}jj$ process is** often referred to as **the golden channel** where to measure VBS properties, for its extremely favourable signal-to-background ratio

- This process is where the first VBS observation was claimed by both collaborations [**ATLAS:** Phys. Rev. Lett. 123 (2019) 161801, **CMS:** PRL 120 (2018) 081801], and now **more interpretations have been added to this channel, leveraging on new analysis techniques and improved background modeling**
  - **Differential (and fiducial) cross section measurements** **(CMS: simultaneous fit with EW $WZjj$ process)**
  - **EFT interpretations**
  - **Polarizations** **(CMS only)**
  - **BSM (Doubly-charged Higgs boson H^{++})**

Analysis strategy

- **Signal regions are very similar to each other in terms of phase space definitions**, therefore the two analyses mainly differ in the MC modeling and object definitions

CMS Signal Region

- $p^T_{\ell_1}(p^T_{\ell_2}) > 25\ (20)$ GeV
- $m_{\ell\ell} > 20$ GeV, $|m_{ee} - m_Z| > 15$ GeV
- $p^T_{miss} > 30$ GeV
- $n_{jets} \geq 2,\ p^T_{j_1},\ p^T_{j_2} > 50$ GeV, no $\mathrm{b_{jets}}$
- $m_{jj} > 500$ GeV, $|\Delta\eta_{jj}| > 2.5$

ATLAS Signal Region

- $p^T_{\ell_1},\ p^T_{\ell_2} > 27$ GeV
- $m_{\ell\ell} > 20$ GeV, $|m_{ee} - m_Z| > 15$ GeV
- $p^T_{miss} > 30$ GeV
- $n_{jets} \geq 2,\ p^T_{j_1}(p^T_{j_2}) > 65\ (35)$ GeV, no $\mathrm{b_{jets}}$
- $m_{jj} > 500$ GeV, $|\Delta y_{jj}| > 2$

Process	ATLAS SR	CMS SR
EW $W^\pm W^\pm jj$	278 ± 30	210 ± 26
QCD $W^\pm W^\pm jj$	27 ± 7	13.7 ± 2.2
Int. $W^\pm W^\pm jj$	8.1 ± 0.7	8.7 ± 2.3
$W^\pm Zjj$	71 ± 8	60.8 ± 8.4
Non-prompt	55 ± 11	193 ± 40
$V\gamma$	13 ± 5	16.5 ± 3.6
Charge misid	11.0 ± 3.5	13.9 ± 6.5
Others	6.7 ± 1.9	5.9 ± 2.1
Total MC	470 ± 40	522 ± 49
DATA	475	524

Fiducial cross sections

- **[ATLAS] Fiducial differential cross sections are extracted from the fit of a 2D template built out of m_{jj} ($m_{\ell\ell}$) and the variable of interest (m_{jj}) [CMS: m_{jj} vs $m_{\ell\ell}$]**

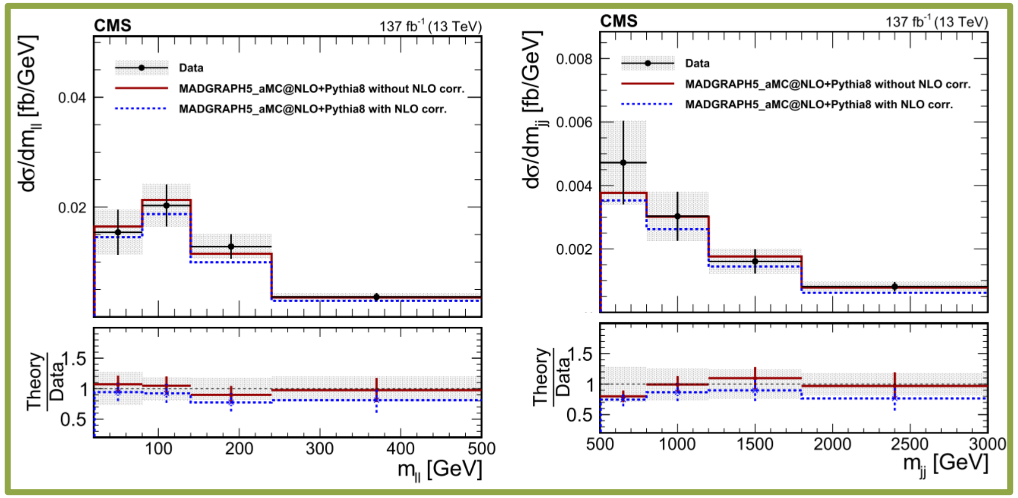

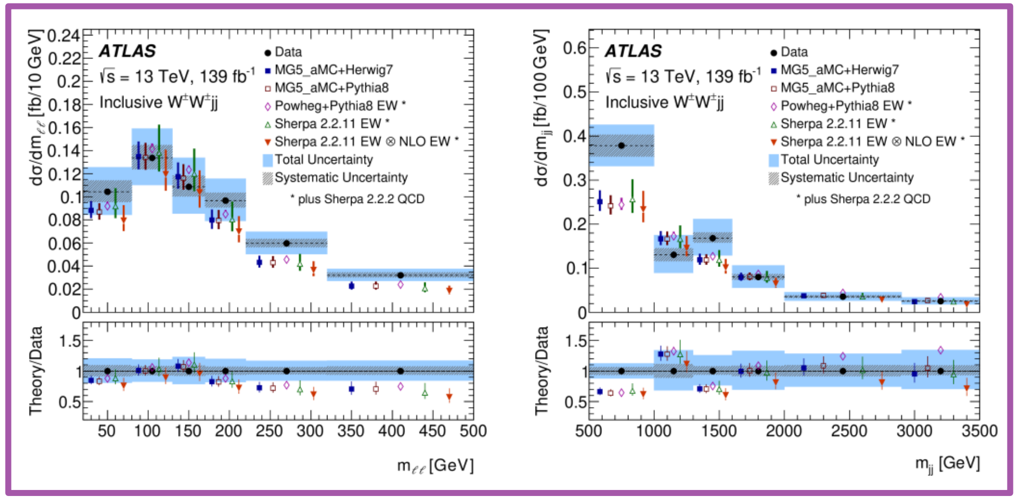

CMS - FIDUCIAL CROSS SECTIONS

Process	$\sigma\,\mathcal{B}$ (fb)	Theoretical prediction without NLO corrections (fb)	Theoretical prediction with NLO corrections (fb)
EW $W^{\pm}W^{\pm}$	3.98 ± 0.45 $0.37\,(\text{stat}) \pm 0.25\,(\text{syst})$	3.93 ± 0.57	3.31 ± 0.47
EW+QCD $W^{\pm}W^{\pm}$	4.42 ± 0.47 $0.39\,(\text{stat}) \pm 0.25\,(\text{syst})$	4.34 ± 0.69	3.72 ± 0.59

ATLAS - FIDUCIAL CROSS SECTIONS

Description	$\sigma_{\text{fid}}^{\text{EW}}$ [fb]	$\sigma_{\text{fid}}^{\text{EW+Int+QCD}}$ [fb]
Measured cross section	2.92 ± 0.22 (stat.) ± 0.19 (syst.)	3.38 ± 0.22 (stat.) ± 0.19 (syst.)
MG5_aMC+Herwig7	2.53 ± 0.04 (PDF) $^{+0.22}_{-0.19}$ (scale)	2.92 ± 0.05 (PDF) $^{+0.34}_{-0.27}$ (scale)
MG5_aMC+Pythia8	2.53 ± 0.04 (PDF) $^{+0.22}_{-0.19}$ (scale)	2.90 ± 0.05 (PDF) $^{+0.33}_{-0.26}$ (scale)
Sherpa	2.48 ± 0.04 (PDF) $^{+0.40}_{-0.27}$ (scale)	2.92 ± 0.03 (PDF) $^{+0.60}_{-0.40}$ (scale)
Sherpa ⊗ NLO EW	2.10 ± 0.03 (PDF) $^{+0.34}_{-0.23}$ (scale)	2.54 ± 0.03 (PDF) $^{+0.50}_{-0.33}$ (scale)
Powheg Box+Pythia	2.64	–

- ATLAS shows several comparisons to theoretical predictions:
  - **MG+P8** and **MG+H7** @LO
  - **SHERPA w/** and **SHERPA w/o** EW corrections @NLO
  - **POWHEG + P8**

Fiducial cross sections

- **[ATLAS] Fiducial differential cross sections are extracted from the fit of a 2D template built out of m_{jj} ($m_{\ell\ell}$) and the variable of interest (m_{jj}) [CMS: m_{jj} vs $m_{\ell\ell}$]**

Source	Impact [%]
Experimental	4.6
Electron calibration	0.4
Muon calibration	0.5
Jet energy scale and resolution	1.9
E_T^{miss} scale and resolution	0.2
b-tagging inefficiency	0.7
Background, misid. leptons	3.4
Background, charge misrec.	1.0
Pile-up modelling	0.1
Luminosity	1.9
Modelling	4.5
EW $W^{\pm}W^{\pm}jj$, shower, scale, PDF & α_s	0.7
EW $W^{\pm}W^{\pm}jj$, QCD corrections	1.9
EW $W^{\pm}W^{\pm}jj$, EW corrections	0.9
Int $W^{\pm}W^{\pm}jj$, shower, scale, PDF & α_s	0.6
QCD $W^{\pm}W^{\pm}jj$, shower, scale, PDF & α_s	2.6
QCD $W^{\pm}W^{\pm}jj$, QCD corrections	0.8
Background, WZ scale, PDF & α_s	0.3
Background, WZ reweighting	1.5
Background, other	1.3
Model statistical	1.8
Experimental and modelling	6.4
Data statistical	7.4
Total	9.8

Source of uncertainty	$W^{\pm}W^{\pm}$ (%)	WZ (%)
Integrated luminosity	1.5	1.6
Lepton measurement	1.8	2.9
Jet energy scale and resolution	1.5	4.3
Pileup	0.1	0.4
btagging	1.0	1.0
Nonprompt rate	3.5	1.4
Trigger	1.1	1.1
Limited sample size	2.6	3.7
Theory	1.9	3.8
Total systematic uncertainty	5.7	7.9
Statistical uncertainty	8.9	22
Total uncertainty	11	23

CMS - FIDUCIAL CROSS SECTIONS

Process	$\sigma\,\mathcal{B}$ (fb)	Theoretical prediction without NLO corrections (fb)	Theoretical prediction with NLO corrections (fb)
EW $W^{\pm}W^{\pm}$	3.98 ± 0.45 $0.37\,(\text{stat}) \pm 0.25\,(\text{syst})$	3.93 ± 0.57	3.31 ± 0.47
EW+QCD $W^{\pm}W^{\pm}$	4.42 ± 0.47 $0.39\,(\text{stat}) \pm 0.25\,(\text{syst})$	4.34 ± 0.69	3.72 ± 0.59

ATLAS - FIDUCIAL CROSS SECTIONS

Description	$\sigma_{\text{fid}}^{\text{EW}}$ [fb]	$\sigma_{\text{fid}}^{\text{EW+Int+QCD}}$ [fb]
Measured cross section	2.92 ± 0.22 (stat.) ± 0.19 (syst.)	3.38 ± 0.22 (stat.) ± 0.19 (syst.)
MG5_aMC+Herwig7	2.53 ± 0.04 (PDF) $^{+0.22}_{-0.19}$ (scale)	2.92 ± 0.05 (PDF) $^{+0.34}_{-0.27}$ (scale)
MG5_aMC+Pythia8	2.53 ± 0.04 (PDF) $^{+0.22}_{-0.19}$ (scale)	2.90 ± 0.05 (PDF) $^{+0.33}_{-0.26}$ (scale)
Sherpa	2.48 ± 0.04 (PDF) $^{+0.40}_{-0.27}$ (scale)	2.92 ± 0.03 (PDF) $^{+0.60}_{-0.40}$ (scale)
Sherpa ⊗ NLO EW	2.10 ± 0.03 (PDF) $^{+0.34}_{-0.23}$ (scale)	2.54 ± 0.03 (PDF) $^{+0.50}_{-0.33}$ (scale)
Powheg Box+Pythia	2.64	–

EFT interpretation

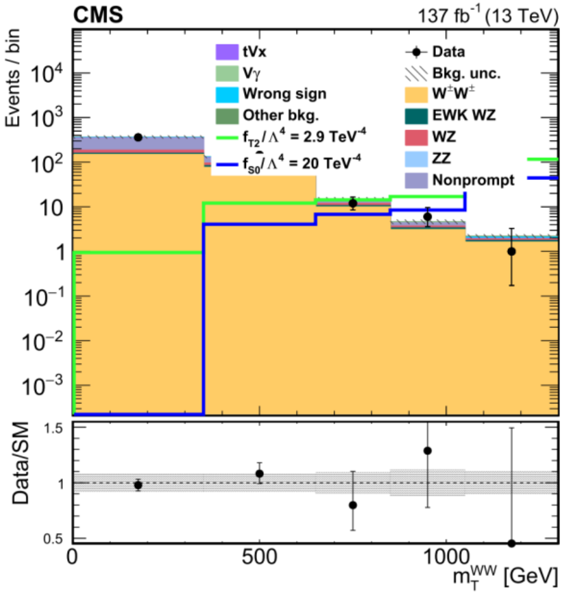

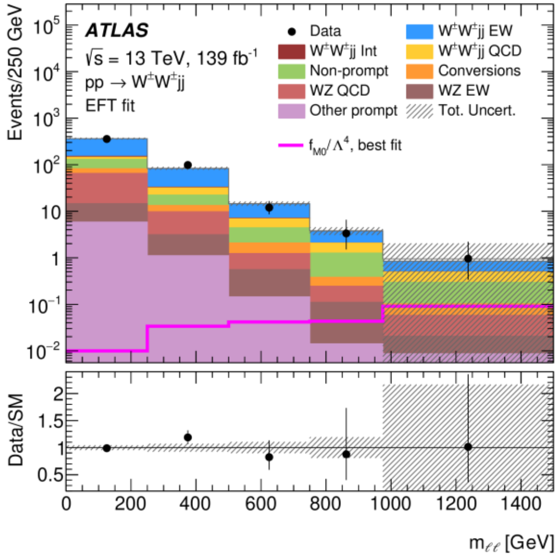

[CMS] D8 EFT operators are constrained by fitting the m_T^{VV} distribution of each channel ($W^\pm W^\pm$ or $W^\pm Z$) ⇒ direct access to the energy scale of the process

[ATLAS] D8 EFT operators are constrained by fitting the $m_{\ell\ell}$ distribution

aQGC	ATLAS (TeV^{-4})	CMS (TeV^{-4})
f_{T0}/Λ^4	$[-0.36, 0.36]$	$[-0.35, 0.37]$
f_{T1}/Λ^4	$[-0.174, 0.186]$	$[-0.16, 0.19]$
f_{T2}/Λ^4	$[-0.63, 0.74]$	$[-0.49\ 0.63]$
f_{M0}/Λ^4	$[-4.1, 4.1]$	$[-3.6, 3.7]$
f_{M1}/Λ^4	$[-6.8, 7.0]$	$[-5.2, 5.5]$
f_{M6}/Λ^4	–	$[-7.2\ 7.3]$
f_{M7}/Λ^4	$[-9.8, 9.5]$	$[-7.8, 7.6]$
f_{S0}/Λ^4	$[-5.9, 5.9]$	$[-5.9, 6.2]$
f_{S1}/Λ^4	$[-23.5, 23.6]$	$[-18, 18]$

2D limits with 2D unitarity bounds on pair of EFT operators of the same group are derived (effect in $EW\ W^\pm Zjj$ taken into account)

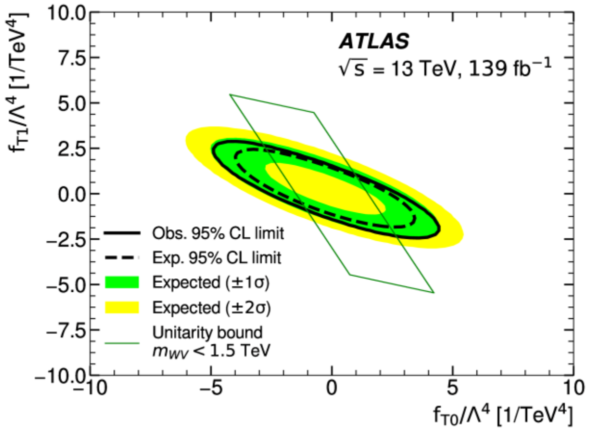

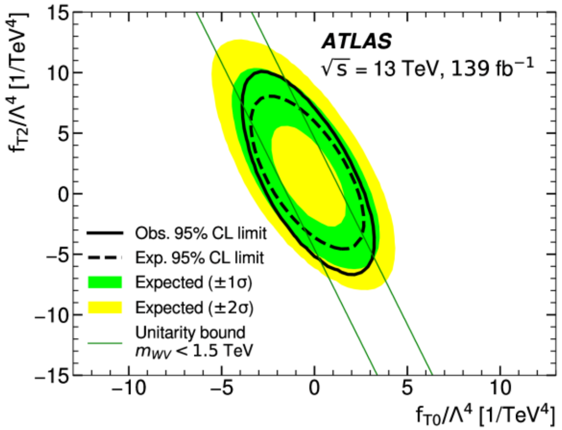

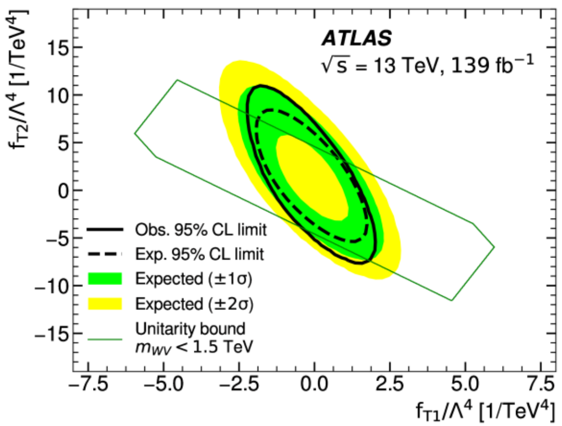

Limits on H^{+}/H^{++} production

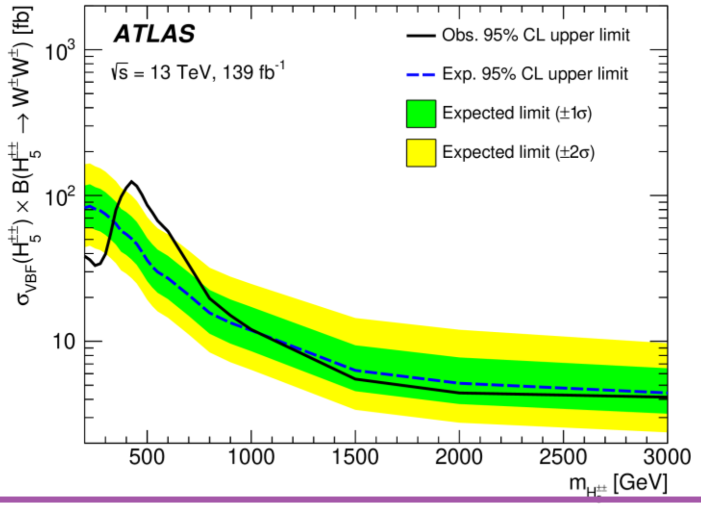

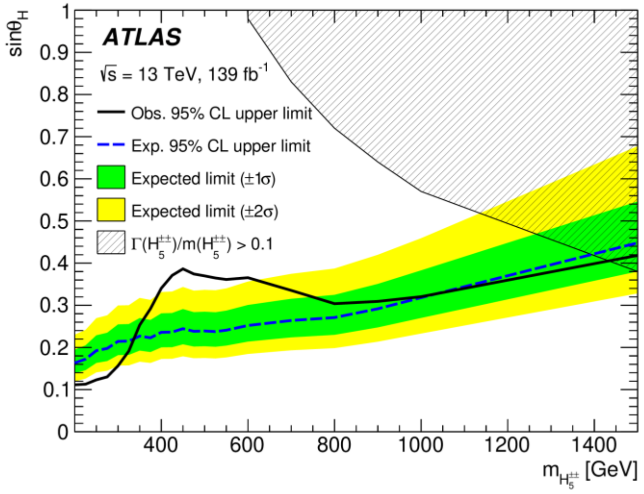

[ATLAS] Doubly-charged Higgs boson interpretation
local excess of 3.3 σ @ 450 GeV, 2.5 σ global

[CMS] Doubly-charged (and single-charged) Higgs boson interpretation excess @ 450 GeV is compatible within 2 σ upward fluctuation

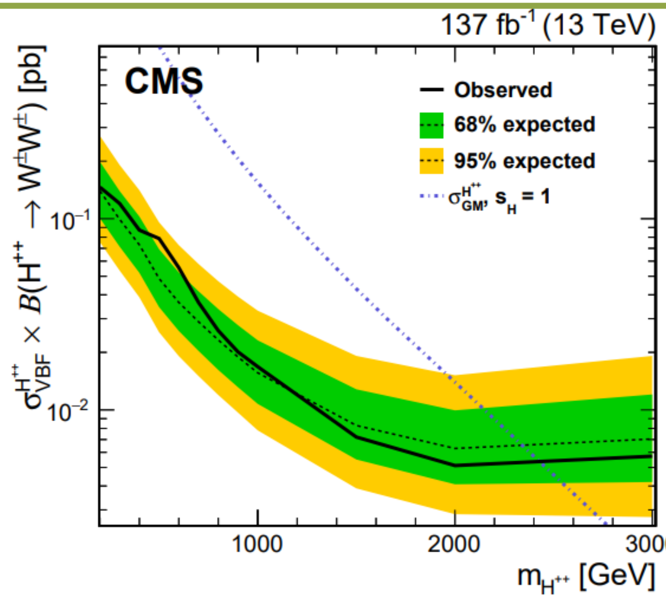

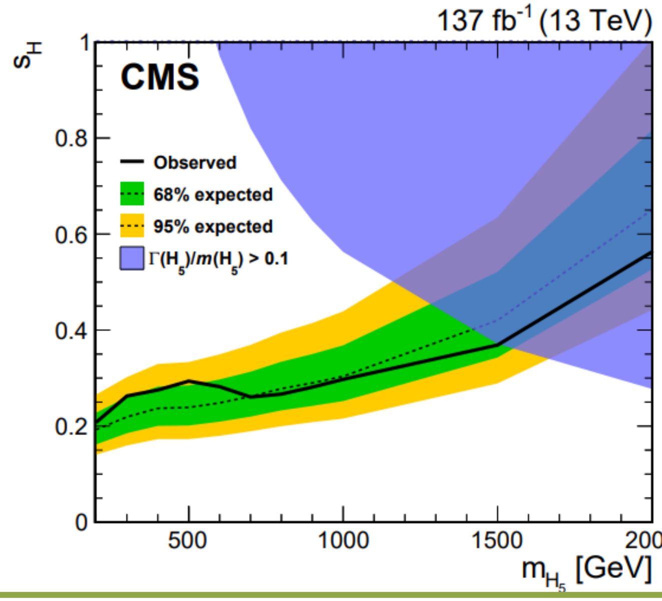

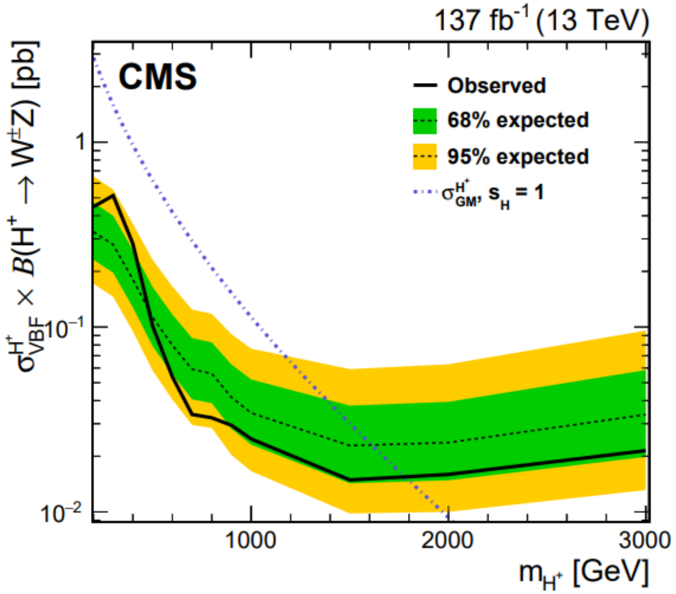

$$W^+W^-jj \rightarrow 2\ell 2\nu jj$$

ATLAS: Submitted to JHEP

CMS: PLB 841 (2023) 137495

$W^+W^-jj \to 2\ell 2\nu jj$

- The EW W^+W^-jj production plays a special role among VBS processes, as the Higgs boson prevents unitarity violation of $W_L W_L \to W_L W_L$ scattering

- Nevertheless, this process poses several experimental challenges, mainly because of the **large $t\bar{t}$ background contamination that enters the signal selection**

- **The ATLAS and CMS collaboration have found the first observation of this process** in the fully leptonic final state (Run 2 data), although two different strategies have been pursued

EW W^+W^-

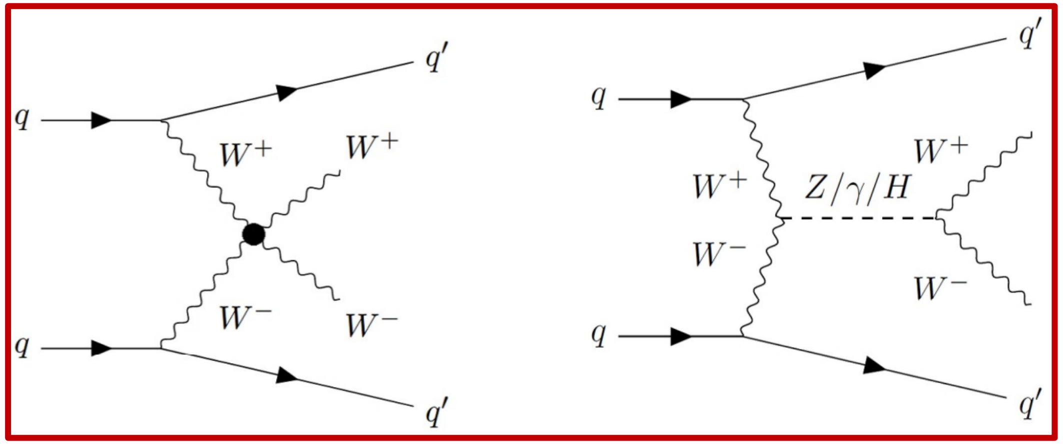

QCD W^+W^-

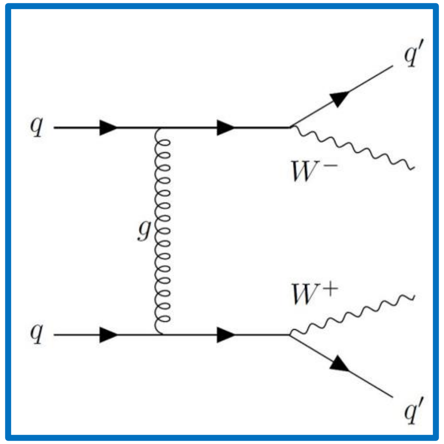

- The signal reconstruction is based on the presence of:
  - ➢ **2 VBS jets**
  - ➢ **2 opposite-charged leptons (either e or μ)**
  - ➢ **Imbalance on the total transverse momentum $\left(p_T^{miss}\right)$**

Event selection

- **Signal regions are substantially diverse from each other in terms of phase space definitions**, and, therefore, difficult to compare – aside from differences in the objects definition

CMS Signal Region

- $p^T_{\ell_1} > 25\ \text{GeV},\ p^T_{\ell_2} > 13\ \text{GeV},\ p^T_{\ell_3} < 10\ \text{GeV}$
- $m_{\ell\ell} > 50\ \text{GeV},\ p^T_{\ell\ell} > 30\ \text{GeV},\ m^T > 60\ \text{GeV}$
- $p^T_{miss} > 20\ \text{GeV}$
- $n_{jets} \geq 2,\ p^T_{j_1},\ p^T_{j_2} > 30\ \text{GeV},\ \text{no b}_{\text{jets}}$
- $m_{jj} > 300\ \text{GeV},\ |\Delta\eta_{jj}| > 2.5$

- $m^T \equiv \sqrt{2 p^T_{\ell\ell} p^T_{miss} \left(1 - cos\,\Delta\phi\,(p^T_{\ell\ell}, p^T_{miss})\right)}$
- $Z_{\ell\ell} \equiv \frac{1}{2}|Z_{\ell_1} + Z_{\ell_2}| = \frac{1}{2}|(\eta_{\ell_1} + \eta_{\ell_2}) - (\eta_{j_1} + \eta_{j_2})|$

ATLAS Signal Region

- $p^T_{\ell_1},\ p^T_{\ell_2} > 27\ \text{GeV},\ p^T_{\ell_3} < 10\ \text{GeV}$
- $m_{e\mu} > 80\ \text{GeV}$
- $p^T_{miss} > 15\ \text{GeV}$
- $n_{jets} = 2 \text{ or } 3,\ p^T_j > 25\ \text{GeV},\ \text{no b}_{\text{jets}}$
- $\zeta > 0.5$

- $\zeta \equiv \min \begin{Bmatrix} [\min(\eta_{\ell_1}, \eta_{\ell_2}) - \min(\eta_{j_1}, \eta_{j_2})], \\ [\max(\eta_{j_1}, \eta_{j_2}) - \max(\eta_{\ell_1}, \eta_{\ell_2})] \end{Bmatrix}$

Signal extraction

- Signal candidates are selected in two SRs:
  - ➢ ***eμ* final state** (dominated by $t\bar{t}$ pair production)
  - ➢ ***ee*/*μμ* final state (**DY + jets events suppressed by imposing $m_{\ell\ell} > 120$ GeV**)**

- The 2 jets ATLAS SR shows a better purity in the very last DNN bin with respect to the CMS DNN

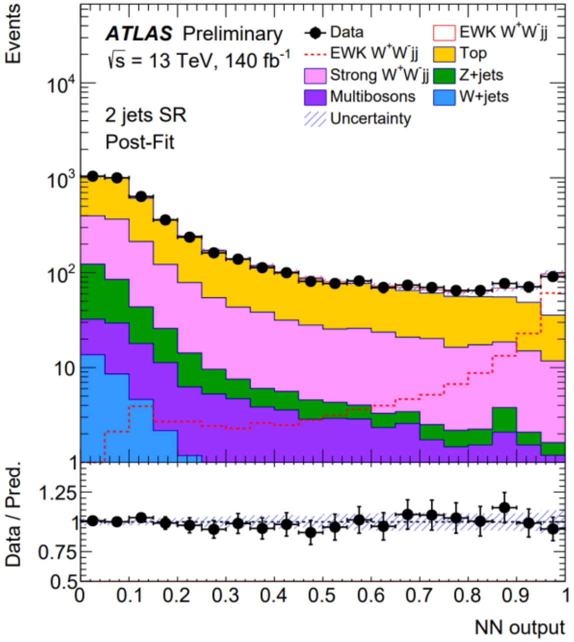

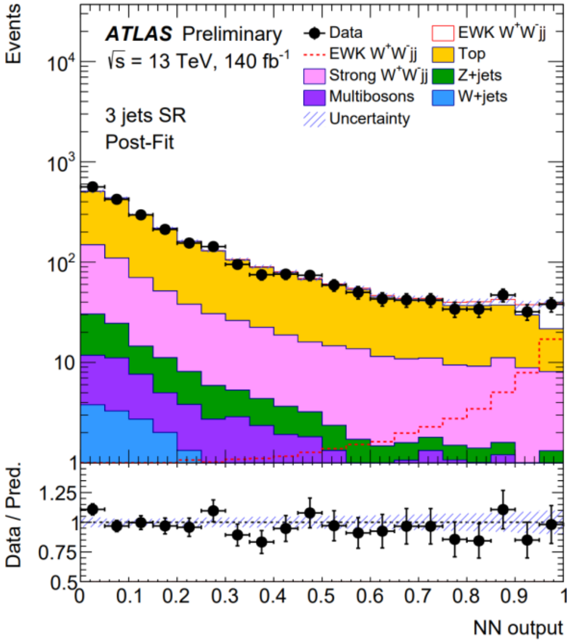

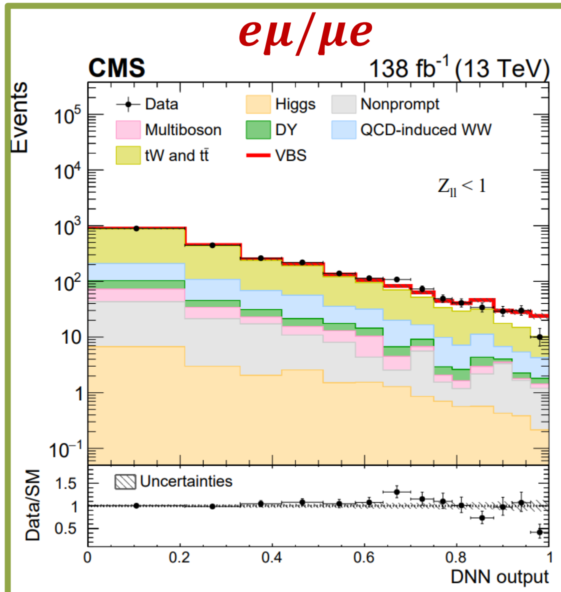

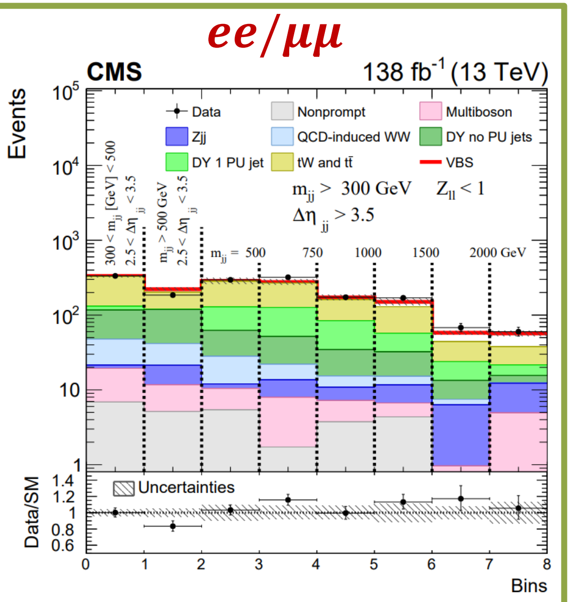

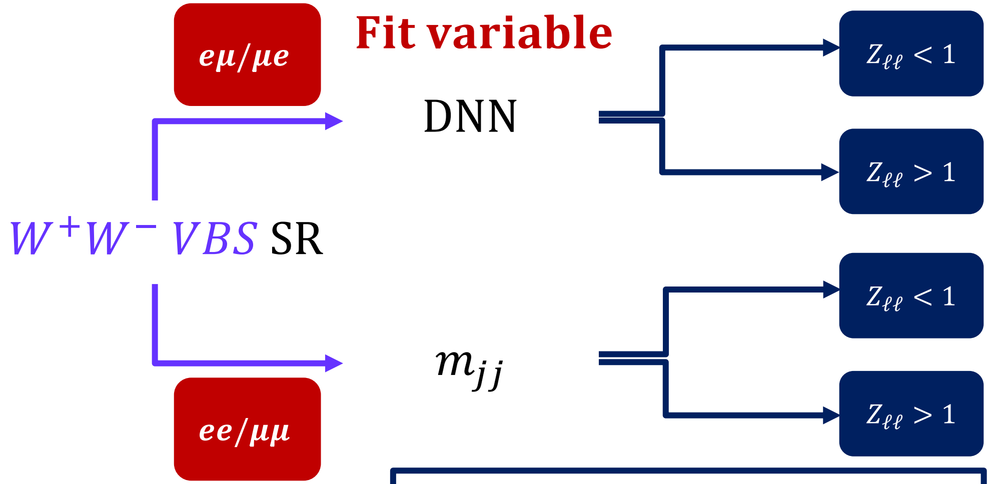

$$Z_{\ell\ell} \equiv \frac{1}{2}\left|(\eta_{\ell_1} + \eta_{\ell_2}) - (\eta_{j_1} + \eta_{j_2})\right|$$

Fiducial cross sections

- Results are extracted to a fiducial phase space where a standard-VBS selection is required on top of the reco-level signal region definition

CMS - FIDUCIAL CROSS SECTION

$e\mu + ee + \mu\mu$

Objects	Requirements
Leptons	$e\mu$, ee, $\mu\mu$ (not from τ decay), opposite charge $p_T^{\text{dressed}\,\ell} = p_T^{\ell} + \sum_i p_T^{\gamma_i}$ if $\Delta R(\ell, \gamma_i) < 0.1$ $p_T^{\ell_1} > 25$ GeV, $p_T^{\ell_2} > 13$ GeV, $p_T^{\ell_3} < 10$ GeV $\lvert\eta\rvert < 2.5$ $p_T^{\ell\ell} > 30$ GeV, $m_{\ell\ell} > 50$ GeV
Jets	$p_T^{j} > 30$ GeV $\Delta R(j, \ell) > 0.4$ At least 2 jets, no b jets $\lvert\eta\rvert < 4.7$ $m_{jj} > 300$ GeV, $\lvert\Delta\eta_{jj}\rvert > 2.5$
p_T^{miss}	$p_T^{miss} > 20$ GeV

Observed significance of 5.6 σ (5.2 σ expected) $e\mu + ee + \mu\mu$ final states

$$\sigma_{fid} = 10.2 \pm 2.0 \text{ fb}$$

MadGraph: $\sigma_{fid}^{theo} = 9.1 \pm 0.6$ fb @LO

ATLAS – FIDUCIAL CROSS SECTION

Category	Requirements
Leptons	$p_T > 27$ GeV and $\lvert\eta\rvert < 2.5$
b-jets	$p_T > 20$ GeV and $\lvert\eta\rvert < 2.5$
Jets	$p_T > 25$ GeV and $\lvert\eta\rvert < 4.5$
Events	One electron and one muon with opposite electric charges No additional lepton $\zeta > 0.5$ $m_{e\mu} > 80$ GeV $E_T^{miss} > 15$ GeV Two or three jets no b-jet $m_{jj} > 500$ GeV **not present @ reco-level**

Observed significance of 7.1 σ (6.2 σ expected) $e\mu$ final state

$$\sigma_{fid} = 2.65^{+0.52}_{-0.48} \text{ fb}$$

POWHEG: $\sigma_{fid}^{theo} = 2.20^{+0.14}_{-0.13}$ fb @NLO

Final considerations

VBS analyses – future directions

- With the large amount of data collected so far by both the ATLAS and CMS collaborations, **several VBS channels have been studied and observed**
  → **What are the next steps?**

  - **Hadronic channels:** not really explored because of their large background contamination but could potentially help in constraining EFT parameters

  - **Run2 + Run 3 analyses:** as most of VBS measurements are still statistically limited, leveraging on the full data delivered by the LHC is how we can further improve results and reduce the largest uncertatinty contribution

  - **Polarization measurements:** the production of longitudinally polarized bosons in VBS processes is very difficult to observe but it gives direct access to the EWSSB mechanism

  - **Channel combination:** the most difficult yet the most promising direction we have to pursue to go deep down in the EW sector of the SM → **VBS global fits can simultaneously constrain different EFT operators by exploiting the sensitivity of each channel to such parameters**

A common framework

- It is evident how comparing different results of the same VBS process is often not trivial and does not allow to easily interpret and combine results → **one could devise a common theoretical framework where to extract fiducial VBS cross sections**

- This was first proposed during the LHC EW WG MB meeting with the aim of providing a shared definition of a fiducial phase space (à-la-STXS) where to extract multiboson results – not strictly confined to VBS measurements

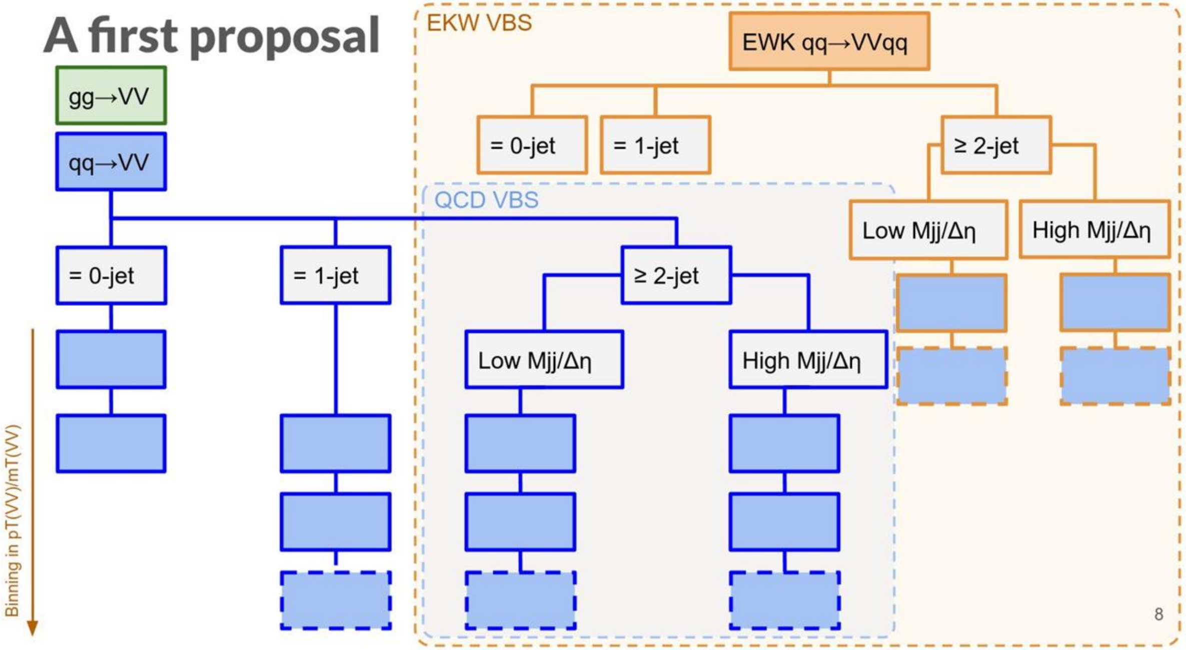

- Project currently under development, need to define particle-level bins and **observables that are sensitive to different channels and/or specific EFT parameters**

- **Allows ATLAS+CMS combinations and facilitate comparisons between experimental results and theory predictions**

Conclusion

- ATLAS and CMS collaborations reported several studies in multiboson channels, **early Run3 results already avaialable and many others are about to come out!**

- VBS processes give direct access to the EW of the SM and are particularly sensitive to BSM effects in the high-energy regime, as they might potentially change couplings between vector bosons
  → **Wide physics program to investigate these mechanism and more data helps to constrain EFT operators**

- Because we have a plethora of multiboson analyses, **it is necessary to define a shared theoretical framework** (like already done in the Higgs sector), which would greatly improve the capability of combining results and facilitate their interpretabitily
  → **positive feedback loop between theorists and the particle physicists community**